Accepted Manuscript

Triazolopyridine Ethers as Potent, Orally Active $mGlu_2$ Positive Allosteric Modulators for Treating Schizophrenia

Mendi A. Higgins, Lawrence R. Marcin, F. Christopher Zusi, Robert Gentles, Min Ding, Bradley C. Pearce, Amy Easton, Walter A. Kostich, Matthew A. Seager, Clotilde Bourin, Linda J. Bristow, Kim A. Johnson, Regina Miller, John Hogan, Valerie Whiterock, Michael Gulianello, Meredith Ferrante, Yanling Huang, Adam Hendricson, Andrew Alt, John E. Macor, Joanne J. Bronson

PII: S0968-0896(16)31181-6
DOI: http://dx.doi.org/10.1016/j.bmc.2016.11.018
Reference: BMC 13385

To appear in: *Bioorganic & Medicinal Chemistry*

Received Date: 29 August 2016
Revised Date: 9 November 2016
Accepted Date: 11 November 2016

Please cite this article as: Higgins, M.A., Marcin, L.R., Christopher Zusi, F., Gentles, R., Ding, M., Pearce, B.C., Easton, A., Kostich, W.A., Seager, M.A., Bourin, C., Bristow, L.J., Johnson, K.A., Miller, R., Hogan, J., Whiterock, V., Gulianello, M., Ferrante, M., Huang, Y., Hendricson, A., Alt, A., Macor, J.E., Bronson, J.J., Triazolopyridine Ethers as Potent, Orally Active $mGlu_2$ Positive Allosteric Modulators for Treating Schizophrenia, *Bioorganic & Medicinal Chemistry* (2016), doi: http://dx.doi.org/10.1016/j.bmc.2016.11.018

Bioorganic & Medicinal Chemistry
journal homepage: www.elsevier.com

Triazolopyridine Ethers as Potent, Orally Active $mGlu_2$ Positive Allosteric Modulators for Treating Schizophrenia

Mendi A. Higgins,* Lawrence R. Marcin, F. Christopher Zusi, Robert Gentles, Min Ding, Bradley C. Pearce, Amy Easton, Walter A. Kostich, Matthew A. Seager, Clotilde Bourin, Linda J. Bristow, Kim A. Johnson, Regina Miller, John Hogan, Valerie Whiterock, Michael Gulianello, Meredith Ferrante, Yanling Huang, Adam Hendricson, Andrew Alt, John E. Macor, Joanne J. Bronson

Bristol-Myers Squibb, Research and Development, 5 Research Parkway, Wallingford, CT 06492-7660, USA

ARTICLE INFO

Article history:
Received
Received in revised form
Accepted
Available online

Keywords:
schizophrenia
$mGlu_2$
metabotropic glutamate receptors
triazolopyridine

ABSTRACT

Triazolopyridine ethers with $mGlu_2$ positive allosteric modulator (PAM) activity are disclosed. The synthesis, *in vitro* activity, and metabolic stability data for a series of analogs is provided. The effort resulted in the discovery of a potent, selective, and brain penetrant lead molecule BMT-133218 ((+)-**7m**). After oral administration at 10 mg/kg, BMT-133218 demonstrated full reversal of PCP-stimulated locomoter activity and prevented MK-801-induced working memory deficits in separate mouse models. Also, reversal of impairments in executive function were observed in rat set-shifting studies at 3 and 10 mg/kg (*p.o.*). Extensive plasma protein binding as the result of high lipophilicity likely limited activity at lower doses. Optimized triazolopyridine ethers offer utility as $mGlu_2$ PAMs for the treatment of schizophrenia and merit further preclinical investigation.

1. Introduction

Schizophrenia is a complex and chronic mental health disorder affecting nearly 1 % of the world's population, including approximately 3.2 million Americans.[1] Consequently, U.S. healthcare expenses related to schizophrenia treatment have been estimated at more than $60 billion annually.[2] The disease usually manifests in early adulthood and usually continues throughout life.[3] While the name is derived from the Greek words for split (schizo) and mind (phrene), sufferers do not have split personalities. Instead, schizophrenia patients present a wide array of positive and negative symptoms along with cognitive deficits that together inflict varying degrees of social and occupational dysfunction.[3] Positive symptoms include hallucinations, delusions, disorganized thought, and movement disorders, while negative symptoms encompass social withdrawal, lack of motivation, reduced pleasure, and flat affect.

The etiology of schizophrenia is not well understood, but it is believed to involve a combination of genetic predisposition and environmental triggers.[4] The standard of care is focused on relieving symptoms through pharmacological intervention, and improving function through psychosocial therapy. Atypical antipyschotics have been the pharmacological treatment of choice since the early 1990s.[5] These drugs work through transient inhibition of dopamine and serotonin receptors in the central nervous system and are reasonably effective at alleviating positive symptoms. Unfortunately, they provide little or no efficacy against negative symptoms and do not improve neurocognitive deficits. Also, these drugs have been associated with multiple side-effects including weight gain, type II diabetes, and hyperlipidemia.[6] Consequently, there is a clear and present need for additional antipsychotic medications that exploit novel modes of action.

A growing body of evidence, including early work with phencyclidine (PCP) and ketamine,[7] has implicated *N*-methyl-D-aspartate (NMDA) receptor hypofunction along with excessive glutamatergic neurotransmission in the pathophysiology of schizophrenia.[8] Consequently, metabotropic glutamate receptor 2 ($mGlu_2$), which is highly expressed in the forebrain and acts as an autoreceptor to diminish glutamate tone, has emerged as an attractive drug target.[9] Activation of this G-protein coupled receptor with exogenous ligands should temper synaptic glutamate levels and alleviate the symptoms and deficits of schizophrenia. Indeed, ground breaking work with a dual $mGlu_{2/3}$ orthosteric agonist LY2140023 (**1**, Figure 1) demonstrated reversal of PCP-induced hyperlocomotion in animal models.[9] Unfortunately, mixed results in clinical trials eventually lead to the discontinuation of **1** in development.[10] Since $mGlu_2$ orthosteric agonists are typically challenged by a lack of mGlu subtype selectivity, poor CNS penetration, and potential for receptor desensitization,[11] many groups have refocused their efforts on positive allosteric modulators (PAMs)

of $mGlu_2$.[12] Unlike agonists, PAMS only potentiate the function of $mGlu_2$ receptors that are activated by endogenous glutamate. This alternative strategy should circumvent receptor desensitization, confer better therapeutic activity, and minimize side-effects. Furthermore, allosteric modulators are likely to exhibit improved CNS penetration since they would not require the polar functionality that is presumably required for binding to the orthosteric site in the receptor. Additionally, $mGlu_2$ selectivity with PAMs should be possible given the likelihood for a less conserved allosteric binding site across receptor subtypes.

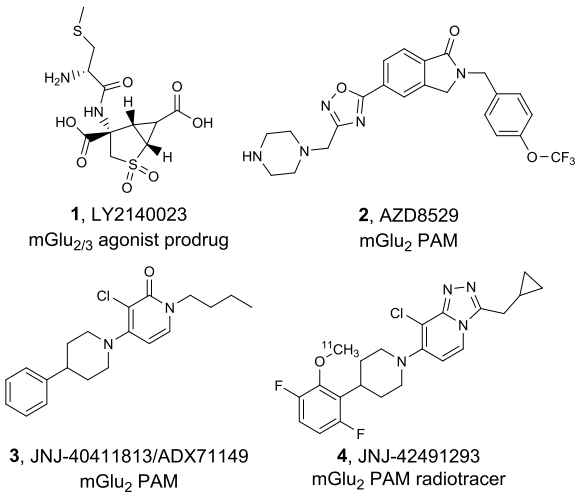

Figure 1. Clinical $mGlu_2$ agents.

Over the past 13 years, a large variety of structurally distinct scaffolds with $mGlu_2$ PAM activity have been disclosed and reviewed in the literature.[13] Two drugs and one PET tracer have been studied in clinical trials. AZD8529 (**2**, Figure 1) was active in seven preclinical models that were used to predict antipsychotic activity.[14] Nevertheless, clinical development of AZD8529 for schizophrenia was abandoned after Phase II studies due to lack of efficacy. In retrospect, the investigators have suggested that an inability to assess target engagement, variable drug exposure, and dose limiting preclinical toxicology findings contributed to the unfavorable outcome.[14,15] Another $mGlu_2$ PAM, JNJ-40411813 (**3**), has demonstrated robust antipsychotic effects in preclinical models and was favorably differentiated from an agonist profile.[16,17] An exploratory study in stably treated patients with schizophrenia suggested that individuals with prominent negative symptoms may have benefited from treatment with JNJ-40411813; however, no additional effect against positive symptoms was reported.[18] As with AZD8529, the investigators have noted that without the capability to confirm $mGlu_2$ target engagement in the clinic, it was uncertain whether sufficient receptor occupancy was achieved.[16] Furthermore, high-dose administration was associated with decreased tolerability. A PET imaging agent, [^{11}C]JNJ-42491293 (**4**) has demonstrated specific and reversible binding to $mGlu_2$ in rat brain and displacement with a $mGlu_2$ PAM.[19] In clinical studies, the PET tracer exhibited radioactivity uptake and washout in striatum and cerebellum, consistent with the distribution of $mGlu_2$ in human brain.[20] It has not been reported if PET tracer **4** shows clinical utility for determining receptor occupancy of $mGlu_2$ PAMs **2** or **3**. Since neither AZD8529 nor JNJ-40411813 were able to unambiguously test the glutamate hypothesis for schizophrenia in clinic trials, there is continued motivation to discover novel $mGlu_2$ PAMs with increased potency and greater tolerability, which can be developed in combination with a useful PET tracer.

Our efforts in the field began with a functional screen of our proprietary compound deck. Over 1 million compounds were assayed for their ability to inhibit forskolin stimulated cAMP production in HEK293 cells stably-expressing human $mGlu_2$. The substituted triazolopyridine (TZP) **5** (EC_{50} = 2.7 uM) was identified from this campaign as an attractive small molecule hit with low micromolar activity (Figure 2). In the course of optimizing the $mGlu_2$ activity of compound **5**, a patent application from Janssen had published disclosing 8-amino-substituted TZPs with $mGlu_2$ PAM activity,[21] including a highly potent phenylpiperidine analog **6** (later identified as JNJ-42153605 with a reported $mGlu_2$ PAM EC_{50} = 17 nM).[22] While this application narrowed novel options to continue working in this space, it also reinforced our desire to exploit untapped opportunities for this privileged scaffold. During our attempts at hit optimization of **5**, we prepared the triazolopyridine ether **7a** as a synthetic intermediate. Interestingly, compound **7a** showed potent $mGlu_2$ activity (EC_{50} = 28 nM, Figure 2) and became the inspiration of a focused drug discovery effort. The following report will disclose $mGlu_2$ PAM structure activity relationships (SARs) for various TZP ether analogs as well as encouraging data in preclinical rodent models of schizophrenia for an advanced lead.

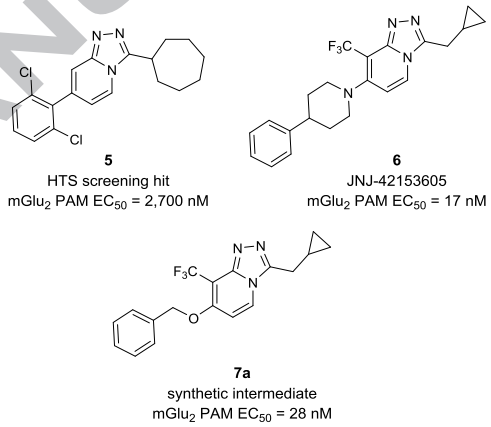

Figure 2. Triazolopyridine-based mGlu2 PAMs**.**

2. Chemistry

As outlined in Scheme 1, a variety of 8-alkyloxy substituted TZP ethers **9a-n** were prepared via copper mediated coupling of primary alcohols with 8-chloro-3-(cyclopropylmethyl)-7-iodo-[1,2,4]-triazolo[4,3-a]pyridine **8**.[22] The yield for this method was typically low (2-10 % yield) due to poor chemoselectivity between halogen atoms. Nonetheless, the procedure was useful for providing small quantities of the desired products for *in vitro* testing. The choice of 8-chloro and 3-(cyclopropylmethyl) substitution of the TZP core was driven by SAR reported for these substituents with structurally related $mGlu_2$ PAMs.[21,22]

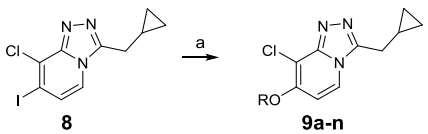

Scheme 1. Reagents and conditions: (a) ROH (7 equiv), copper(I) iodide (2 equiv), 1,10-phenanthroline (1.2 equiv), cesium carbonate (1.8 equiv), toluene, 100 ^{o}C, 17-24 h, 2-10 % yield. For the structures of compounds **9a-n**, refer to Table 1.

Additional TZP ethers bearing a C-8 trifluoromethyl group were made using alternative methods (Scheme 2). For this set of analogs, focus was given to the hydrophobic ether side chains

that had substitution at likely metabolic softspots and/or possessed some element of conformational restriction. Compounds **7a, b, e-m** were prepared in 4 steps and good overall yield as shown in Scheme 2. Chlorine displacement in 2,4-dichloro-3-trifluoromethyl pyridine **10**[22] with commercially available or readily obtained alcohols afforded ethers **11** with complete regioselectivity. Hydrazine displacement of the second chlorine atom provided hydrazine adducts **12**. Acylation with cyclopropylacetyl chloride followed by mild cyclodehydration using the Burgess reagent afforded the final products in good overall yield. Chiral separation of racemic **7m** using supercritical fluid chromotography (SFC) provided the pure enantiomers (+)-**7m** and (-)-**7m**. The absolute configuration of (+)-**7m** was assigned 1*S*,2*S* through single crystal X-ray analysis using heavy atom techniques.[23]

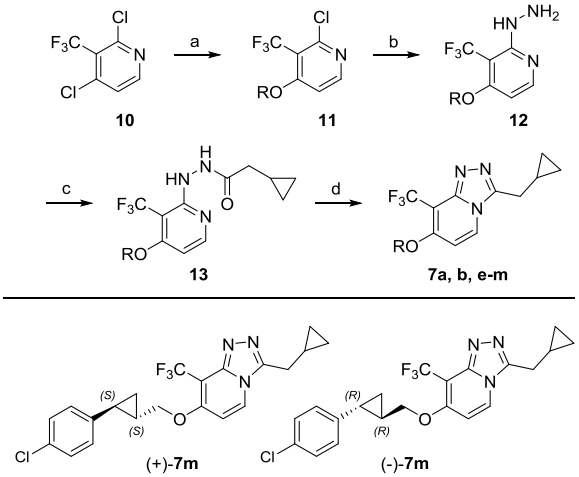

Scheme 2. Reagents and conditions: (a) ROH, NaH, DMF, 0 ºC, 1 h, ~70%; (b) NH_2NH_2, dioxane, 95 ºC, 1 h, quantitative yield; (c) cyclopropylacetyl chloride, TEA, CH_2Cl_2, 0 ºC, 1 h; (d) Burgess reagent, dioxane/acetonitrile, 85 ºC, 12 h, 9-65 % (over two steps). For the structures of compounds **7a, b, e-m**, refer to Table 2.

Obviating the need for chiral separation, cyclopropylmethyl ether (+)-**7m** was also synthesized using ((1*S*,2*S*)-2-(4-chlorophenyl)cyclopropyl)methanol (**17**, Scheme 3). The homochiral alcohol **17** was made from (*E*)-3-(4-chlorophenyl)acrylic acid (**14**) via diastereroselective palladium–catalyzed cyclopropanation of the (+)-camphorsultam acrylamide **15**, followed by lithium aluminum hydride reduction (Scheme 3). The diastereoselectivity of the cyclopropanation event was greater than 95% diastereomeric excess (de) and was further enriched to greater than 99 % de after silica gel column chromatography of intermediate **16**. An X-ray crystal structure of **16** confirmed the stereochemistry of the newly formed cyclopropane as 1*S*,2*S*.[24] Alcohol **17** was converted to (+)-**7m** via the methods outlined in Scheme 2.

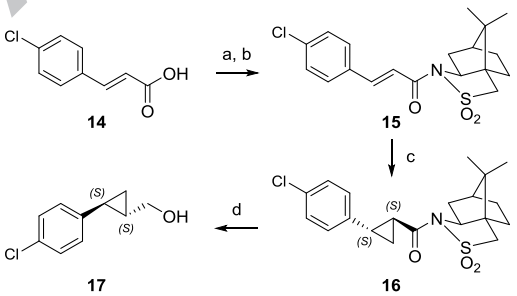

Scheme 3. Reagents and conditions: (a) thionyl chloride, DCM, reflux, 24 h, quantitative yield; (b) (3a*R*,6*R*,7a*S*)-8,8-dimethylhexahydro-1H-3a,6-methanobenzo[c]isothiazole 2,2-dioxide, TEA, DCM, 0 ºC, 82 % yield; (c) N-methyl-N'-nitro-N-nitrosoguanidine, $Pd(OAc)_2$, -10 ºC, DCM, 73 % yield; (d) LAH, THF, -40 ºC, 1 h, 99 % yield.

A more convergent palladium catalyzed etherification strategy was used to prepare TZP ethers **7c** and **7d** from intermediate **18** (Scheme 4). The use of JOSIPHOS as a ligand for palladium was critical to the success of this coupling procedure. It should be noted that an excess of primary alcohol was necessary to achieve yields of up to 20 %. Also, secondary alcohols were unreactive under these conditions.

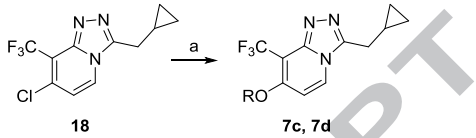

Scheme 4. Reagents and conditions: (a) ROH (5 equiv), JOSIPHOS (0.2 equiv), Cs_2CO_3 (2 equiv), allylpalladium (II) chloride dimer (0.1 equiv), toluene, 135 ºC, 3 h, 13-20 % yield. For the structures of compounds **7c** and **7 d**, refer to Table 2.

3. Results

3.1. In Vitro Characterization

The $mGlu_2$ functional activity for 8-chloro TZP ethers **9a-n** is detailed in Table 1. The simple benzyl ether **9a** exhibited modest, yet encouraging, $mGlu_2$ functional activity (EC_{50} = 180 nM). Single chlorine substitution of the benzylic ring at the *ortho*-, *meta*-, and *para*-positions provided a 3-16 fold improvement in activity as evidenced by compounds **9b-d**. The ortho and meta isomers **9c** and **9d** were both more potent (EC_{50} = 17 nM and 11 nM, respectively) than the para isomer (EC_{50} = 60 nM). A slightly larger increase in potency was observed with the corresponding isomeric biphenyls **9e-g**. In contrast to the chloro analogs, the para substitution pattern of **9e** was preferred (EC_{50} = 6.8 nM). The naphthalene **9h** and tetrahydronapthalene **9i** derivatives also maintained high levels of functional activity (EC_{50} = 29 nM and 18 nM, respectively). Incorporation of polar basic functionality in the form of a pyridine, pyrimidine, or isoquinoline was not tolerated as demonstrated by compounds **9j-m**. Interestingly, the homologated phenethylether **9n** also gained ~6 fold improvement in activity over the benzyl ether **9a**. A significant issue across the series was moderate to rapid in vitro metabolism in human, rat, and mouse liver microsomes (HLM, RLM, and MLM, respectively). Percent of drug remaining after a 10 minute incubation with RLM and MLM was typically low. Biotransformation studies of representative analogs with liver microsomes and freshly prepared rat hepatocytes revealed that *O*-dealkylation of the benzyl ether in our analogs was the major route of metabolism. Glutathione displacement of the 8-chlorosubstitutent was also observed and considered to be a significant liability. In order to curb metabolism and avoid reactive metabolite formation, subsequent efforts to build additional SAR was carried out with the C-8 trifluoromethyl group on the TZP core.

Table 1
Functional $mGlu_2$ potency and metabolic stability of TZP ethers **9a-n**.

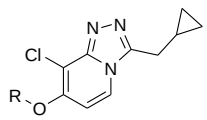

cmpd	R	$mGlu_2$ PAM EC_{50}, nM (Glu max)[a]	HLM, RLM, MLM (% remaining)[b]
9a	benzyl	180(100%)	74, 39, 32
9b	4-chlorobenzyl	60(94%)	79, 52, 47
9c	3-chlorobenzyl	17(97%)	77, 34, 52
9d	2-chlorobenzyl	11(99%)	65, 15, 16

9e	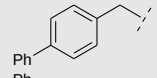	6.8(95%)	83, 50, 55
9f	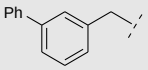	13(95%)	13, 0.1, 0.2
9g	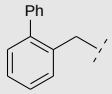	20(95%)	45, 0.1, 0.2
9h	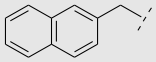	29(96%)	80, 27, 3
9i	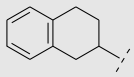	18(96%)	49, 15, 0.3
9j	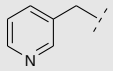	>15,000(nd)	93, 48, 37
9k	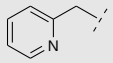	>3,000(nd)	80, 83, 75
9l	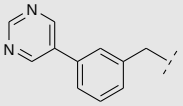	720(95%)	57, 18, 30
9m	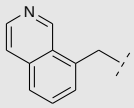	230(97%)	44, 3, 2
9n	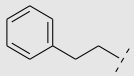	32(101%)	73, 13, 4

[a] EC_{50} values represent functional activity for inhibition of forskolin stimulated cAMP production in HEK293 cells stably-expressing human $mGlu_2$. Values are mean of ≥ 2 experiments. [b]In vitro metabolic stability in human, rat, and mouse liver microsomes. Results are expressed as % remaining after 10 min incubation.

In vitro data for C-8 trifluoromethyl TZP ethers **7a-m** is detailed in Table 2. The benzyl ether **7a** was 6 fold more potent than the corresponding C-8 chloro analog **9a**, but microsomal stability was still poor in RLM and MLM. While *in vitro* potency of variously substituted phenethylethers **7b-h** was encouraging (EC_{50} = 1.8-16 nM), microsomal stability was highly dependent on the nature of substitution. Neither the geminal difluoro analog **7b** nor α-methyl compound **7c** showed differentiated metabolism. Dimethyl analogs **7d-e** and cycloalkyl derivatives **7f-h** demonstrated a significant improvement in percent remaining after 10 min incubation with liver microsomes. The most promising category of compounds was the ring constrained ethers **7i-m**. Phenylcyclohexyl and phenylcyclobutyl ethers **7i** and **7j** both displayed subnanomolar $mGlu_2$ PAM activity (EC_{50} = 0.4-0.5 nM). Metabolic stability of the cyclohexane **7i** was significantly better than the cyclobutane **7j,** but improvements with the latter were realized with 4-fluorophenyl substitution (compound **7k**). The racemic trans-methylcyclopropanes **(**±**)-7l** and (±)-**7m** exhibited excellent $mGlu_2$ activity (EC_{50} = 1.3-1.7 nM). Metabolic stability of the 4-chloro isomer (±)-**7m** in rodent liver microsomes was marginally better than the 4-fluoro congener **(**±**)-7l**. This prompted characterization of the separated enantiomers (+)-**7m** and (-)-**7m**. The dextrorotatory isomer (+)-**7m**, with an absolute configuration of 1*S*,2*S*, showed 3-4 fold greater $mGlu_2$ activity than the 1*R*,2*R* enantiomer (-)-**7m**. In contrast to prior results with 8-chloro TZP analogs, reactive metabolites were not observed in biotransformation studies with the 8-trifluoromethyl TZP (+)-**7m**. Given the encouraging in vitro data for **(+)-7m** (also referred to as BMT-133218), we embarked on a more in-depth characterization of this interesting lead.

Table 2
Functional $mGlu_2$ potency and metabolic stability of TZP ethers **7a-m**.

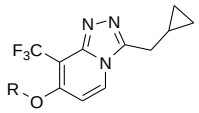

cmpd	R	$mGlu_2$ PAM EC_{50}, nM (Glu max)[a]	HLM, RLM, MLM (% remaining)[b]
7a	benzyl	28(92%)	80, 10, 24
7b	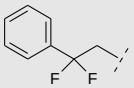	6.1(95%)	72, 47, 22
7c	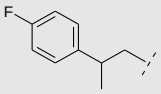	10(97%)	40, 8, 12
7d	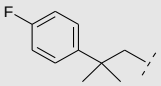	11(97%)	90, 79, 49
7e	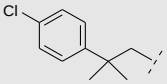	5.5(94%)	91, 79, 47
7f	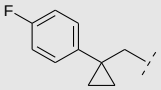	16(94%)	83, 57, 55
7g	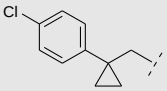	13(92%)	77, 63, -
7h	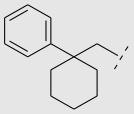	1.8(95%)	15, 0.8, 21
7i	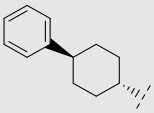	0.4(94%)	85, 75, 83
7j	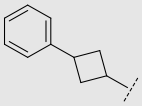	0.5(98%)	72, 36, 27
7k	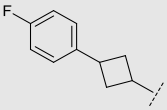	0.4(100%)	83, 69, 60
7l	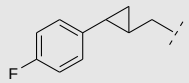	1.7(96%)	79, 53, 46
7m	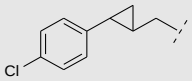	1.3(96%)	76, 83, 60
(+)-7m	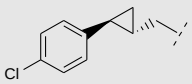	1.4(99%)	83, 84, 74
(-)-7m	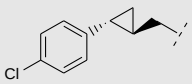	4.0(96%)	92, 79, 52

[a] EC_{50} values represent functional activity for inhibition of forskolin stimulated cAMP production in HEK293 cells stably-expressing human $mGlu_2$. Values are mean of ≥ 2 experiments. [b]In vitro metabolic stability in human, rat, and mouse liver microsomes. Results are expressed as % remaining after after 10 min incubation.

In alignment with its robust functional activity, BMT-133218 demonstrated potent binding affinity (Ki = 1.0 nM) for the allosteric site of $mGlu_2$ in a competition binding assay using the PAM radioligand [^{3}H]-JNJ-40068782 (Table 3).[25] BMT-133218 also exhibited > 600-fold functional selectivity for the reduction of cAMP levels in cells overexpressing human $mGlu_2$ versus human $mGlu_3$. To more definitively determine that BMT-133218 functioned as a PAM at $mGlu_2$, it was evaluated in a humanized

monkey $mGlu_2$ Gqi5 FLIPR assay. When glutamate dose response curves were run in the presence of increasing concentrations of BMT-133218, a "left-shift" of greater than 18-fold was observed for the EC_{50} of glutamate, Figure 3.[26] When the FLIPR assay was carried out in agonist mode (no added glutamate), BMT-133218 displayed a low level of $mGlu_2$ agonist activity ($mGlu_2$ agonist EC_{50} = 530 nM).

Table 3
In vitro characterization of **(+)-7m** (BMT-133218).

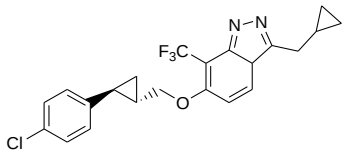

cmpd	$mGlu_2$ PAM EC_{50} (nM)[a]	$mGlu_3$ PAM EC_{50} (nM)[a]	$mGlu_2$ binding Ki (nM)[b]	$mGlu_2$ FLIPR PAM fold-shift[c]	$mGlu_2$ FLIPR agonist EC_{50} (nM)[c]
(+)-7m	1.4 ± 1.1	890 ± 230 [d]	1.0 ± 0.3	> 18	530 ± 220 [e]

[a] Inhibition of forskolin-stimulated cAMP production in HEK293 cells stably-expressing human $mGlu_2$ or human $mGlu_3$. Values are mean of ≥ 2 experiments. [b]Radioligand competition experiment using HEK293 cell membrane homogenates and the PAM radioligand [^{3}H]-JNJ-40068782. [c]Humanized monkey $mGlu_2$ FLIPR assay. [d]mGlu3 max = 76%. [e]mGlu2 max = 85%.

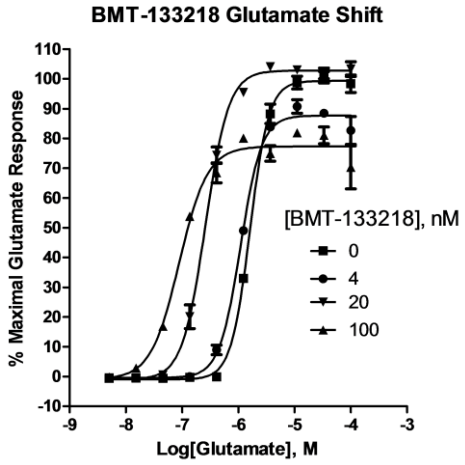

Figure 3. Humanized monkey $mGlu_2$ FLIPR glutamate shift assay results for (+)-**7m** (BMT-133218), n = 4.

3.2. Physiochemical Properties and Pharmacokinetics

A summary of physiochemical properties for BMT-133218 is presented in Table 4. The mass of 421 Daltons is slightly above the average of 357 Daltons for all marketed neuroscience drugs.[27] The calculated LogP and experimentally determined HPLC LogD values of 4.4 and 4.7, respectively, suggested lipophilic character approaching the high end of ideal drug properties. The consequence of high lipophilicity was reflected in extensive protein binding (> 99.4 %) across species and low aqueous solubility at neutral pH (~2 ug/mL @ pH 6.5).

Table 4
Physiochemical properties of **(+)-7m** (BMT-133218).

cmpd	MW (Daltons)	cLogP[a] value	exptl. LogD[b] value	plasma protein binding hum/rat/mouse (% free)	aqueous solub. @ pH 6.5 (μg/mL)
(+)-7m	421	4.4	4.7	0.2/0.6/0.5	2

[a]Calculated using Chem Axon software. [b]Determined through application of published HPLC methods. [c]Thermodynamic solubility of crystalline material in 50 mM phosphate buffer.

Pharmacokinetic data for BMT-133218 in male Sprague-Dawley rats is summarized in Table 5. After oral administration at 3 mg/kg, BMT-133218 displayed a plasma C_{max} of 4.1 μM at 2.7 hours post dose and an AUC_{0-24} of 39 μM*h. A brain/plasma ratio of 0.38 was observed 1 hour post dose in a separate rat brain uptake experiment. Brain uptake in C57B1/6 mice (10 mg/kg, *p.o.*) was very similar (b/p_{mouse} = 0.46) to the rat. Despite apparent challenges in physiochemical properties, it was anticipated that good pharmacokinetics and high target potency observed with BMT-133218 would be sufficient to drive pharmacodynamic effects in animal models of schizophrenia.

Table 5
PK and brain uptake data for compound **(+)-7m** (BMT-133218) after oral administration at 3 mg/kg in Sprague-Dawley Rats.

cmpd	C_{max} (μM)[a]	T_{max} (h)[a]	AUC_{0-24} (μM*h)[a]	plasma (μM)[b]	brain (μM)[b]	brain/ plasma[b]
(+)-7m	4.1 ± 0.2	2.7 ± 0.6	39.4 ± 0.4	3.6 ± 0.5	1.4 ± 0.2	0.38

[a]Values are the mean of three animals. [b]Plasma and brain concentrations determined after 1 h of a single dose at 3 mg/kg. [c]10% DMSO/18% TPGS/ 72% water

3.3. In Vivo Efficacy

BMT-133218 was tested for its ability to inhibit phencyclidine-induced hyperlocomotion (PCP-LMA) in mice. This model is widely used as an in vivo screen for novel antipsychotics due to its sensitivity to many typical and atypical antipsychotics. This assay is also well-suited for testing $mGlu_2$-based mechanisms, as PCP stimulates an excess of glutamate release coincident with locomotor hyperactivity. Mice treated with BMT-133218 dosed at 10 mg/kg (*p.o.*) demonstrated a statistically significant reduction in locomotor activity after PCP administration when compared to animals that received PCP alone (Figure 4). BMT-133218 dosed at 3 mg/kg (*p.o.*) showed a non-significant trend for reversal. The positive control, risperidone, was fully effective in reducing hyperlocomotion in the same study. Plasma and brain drug concentrations from satellite animals dosed with BMT-133218 at 10 mg/kg (*p.o.*) and harvested at a time corresponding to the peak PCP response (1 hour) were 15.4 uM and 6.8 uM, respectively. The mice dosed at 3 mg/kg had proportionally lower exposures. Brain to plasma ratios were similar across dose groups (b/p = 0.35-0.44) and consistent with prior brain uptake experiments in mice. The calculated free plasma drug concentrations at 10 and 3 mg/kg were 76 and 21 nM, respectively.

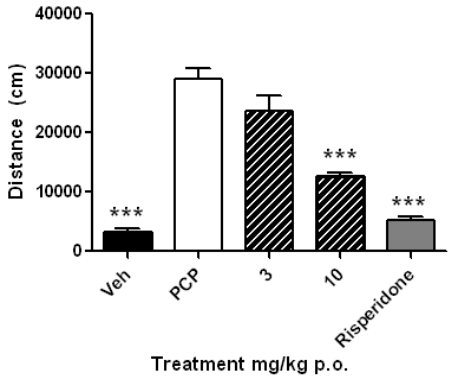

cmpd	dose (mg/kg)[a]	behavioral efficacy	plasma (μM)[b]	brain (μM)[b]	brain/ plasma	free drug plasma (nM)[c]
(+)-7m	3	No	4.2 ± 0.3	1.5 ± 0.4	0.35	21
(+)-7m	10	Yes	15.4 ± 0.3	6.8 ± 0.4	0.44	76

[a]Drug samples were prepared in 10% DMSO/18% TPGS/72% water and dosed orally 30 minutes prior to PCP treatment (3.2 mg/kg, *s.c.*). Risperidone was prepared in 0.3% tartaric acid. [b]Values are the mean of three animals from satellite group. [c]Assuming 99.5% protein binding in mouse plasma.

Figure 4. In vivo dose response of **(+)-7m** (BMT-133218) at 3 and 10 mg/kg (*p.o.*) in PCP-stimulated locomotion studies using C57B1/6J male mice. Locomotor activity is expressed as the mean of total distance travelled (n= 14-16/group) during the 2 h post-PCP administration. Data were analyzed by one-way ANOVA followed by Dunnet's test; *** $p < 0.001$ versus Veh/PCP treatment. Risperidone was used as a positive control.

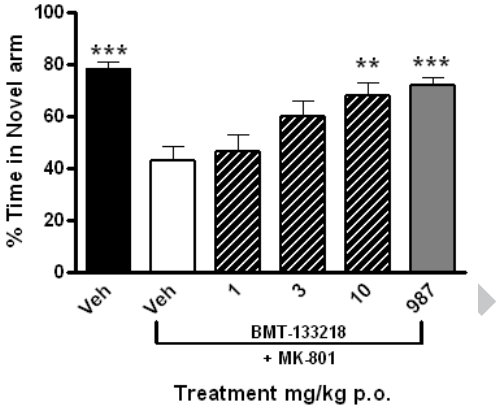

cmpd	dose (mg/kg)	efficacy	plasma (μM)[a]	brain (μM)[a]	brain/ plasma	free plasma (nM)
(+)-7m	1	No	0.84 ± 0.18	0.24 ± 0.05	0.29	4
(+)-7m	3	No	2.2 ± 0.3	0.63 ± 0.9	0.35	11
(+)-7m	10	Yes	8.2 ± 1.0	4.1 ± 1.0	0.44	41

[a]Values are the mean of three animals from satellite groups. [c]Assuming 99.5% protein binding in mouse plasma.

Figure 5. Dose response of BMT-133218 or **(+)-7m** in two-trial Y-maze experiment. Results from the free-choice trial are presented as the mean % time spent in the novel arm ± SEM (n = 14-16/treatment group) and were analyzed by one-way ANOVA followed by Dunnett's test; ** P<0.01, *** P<0.001 versus Veh/Mk-801 treatment. PNU-282987 (987) was used as a positive control.

The effects of BMT-133218 on two-trial Y-maze performance in MK-801 treated mice are shown in Figure 5. The Y-maze assay is commonly used to evaluate novel chemical entities for their effects on working memory. The test measures a rodent's preference to investigate a new arm of the maze during a free choice trial rather than returning to one that was previously visited during the forced choice trial, indicating recognition of the previously visited arm. MK-801 is a nonselective NMDA receptor antagonist that imparts cognitive deficits in this model. In the study, mice treated with vehicle showed a strong preference for the novel arm. In contrast, mice treated with MK-801 (0.05 mkg/kg, s.c.) spent an equivalent amount of time in each arm. Animals treated with BMT-133218 at 10 mg/kg (p.o.), 30 minutes prior to MK-801 administration and 60 min prior to the forced choice trial, demonstrated a significant increase in time spent in the novel arm. Animals treated with 3 mg/kg BMT-133218 showed a trend toward reversing MK-801-induced cognitive deficits, but the results did not reach statistical significance. The effective dose of 10 mg/kg showed comparable activity to the positive control, the α7 nACh receptor full agonist PNU-282987.[28] Exposure data for BMT-133218 from satellite animals revealed dose-proportional drug concentrations in brain and plasma, and an average unbound drug plasma level of 41 nM for animals receiving the active dose of 10 mg/kg.

BMT-133218 was also evaluated at oral doses of 1, 3, and 10 mg/kg for its ability to reverse MK-801 deficits in the rat maze-based set-shifting paradigm (Figure 6).[29] The induced impairment in attentional set-shifting parallels deficits observed on tests of executive function in schizophrenia patients and can serve as a useful preclinical tool in rats for measuring prefrontal cortical function. In this assay, results are expressed as the number of trials to reach performance criterion during the set-shift task. Rats receiving MK-801 (0.04 mg/kg, *i.p.*) 35 minutes prior to the set-shift task required significantly more trials to reach criterion compared to rats that only received vehicle (saline) injection. Conversely, rats that received the well characterized α7 nAch receptor partial agonist SSR180771,[30] immediately prior to MK-801 treatment, demonstrated a significantly reduced number of trials to reach performance criterion compared to the MK-801 only treated group. BMS-133218 demonstrated a statistically significant reduction in trials at oral doses of 3 and 10 mg/kg, but not at 1 mg/kg. Brain and plasma samples from BMT-133218 treated satellite animals were used to project drug exposure during the set-shift experiment. Again, drug exposure was dose-proportional and brain-to-plasma ratios were in close alignment with other experiments. Animals receiving the active dose of 3 and 10 mg/kg of BMT-133218 had free drug plasma concentrations of 230 and 610 nM at 1 hour after oral administration, respectively.

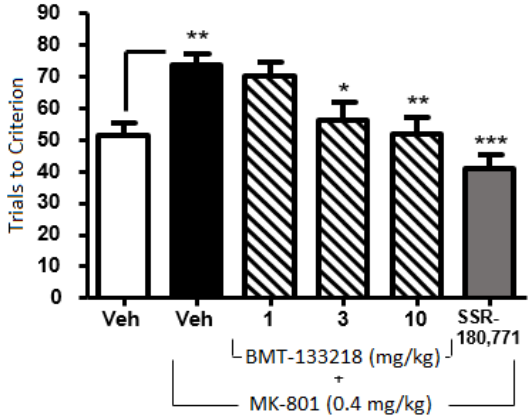

cmpd	dose (mg/kg)	efficacy	plasma (μM)[a]	brain (μM)[a]	brain/ plasma	free drug plasma (nM)
(+)-7m	1	No	1.1 ± 0.7	0.7 ± 0.5	0.66	63
(+)-7m	3	Yes	3.8 ± 0.2	1.5 ± 0.3	0.40	230
(+)-7m	10	Yes	10 ± 2	5.8 ± 0.4	0.59	610

[a]Values are the mean of three animals from satellite group. [c]Assuming 99.4% protein binding in rat plasma.

Figure 6. Effect of **(+)-7m** (BMT-133218) on set-shifting performance in rat. Results are expressed as the number of trials to meet criterion (n = 8) and were analyzed by one way ANOVA followed by Dunnett's test; * $p<0.05$, ** $p<0.01$, *** $p<0.001$ versus Veh/MK-801. SSR180,771 was used as a positive control. Saline was used as the vehicle.

4. Molecular Modeling

BMT-133218 and JNJ-42153605 only differ in substitution at the C7 position of the triazolopyridine core. To better understand the shared pharmacophore of the corresponding cyclopropylmethyl ether and phenylpiperidine substituents, a computational study was performed.[31] JNJ-42153605 was conformationally sampled to find the global minimum and a set of local minima within 3.5 kcal/mol. The same analysis was done with BMS-133218. The two molecules with all of their minima were overlayed on the central heterocycle. The global minimum of JNJ-42153605 adopts an extended conformation and is shown in yellow in Figure 7. In contrast, the global minimum of BMT-133218, shown in purple, is collapsed on itself and gains intramolecular hydrophobic contacts and π-stacking interactions. The striking difference in global minima can be attributed to the presence of 2 additional rotatable bonds in the ether side chain of BMT-133218, allowing increased conformational flexibility. Nevertheless, a low energy conformer of BMT-133218, shown in blue, that is within 2.7 kcal/mol of the global minimum overlays nicely with the global minimum of JNJ-42153605. The energy cost for BMT-133218 to adopt this extended conformation may be partially off-set via interaction with the hydrophobic mGluR2 allosteric binding pocket.

5. Discussion and Conclusions

BMT-133218 resulted from optimization of the $mGlu_2$ functional activity and *in vitro* metabolic stability of our novel triazolopyridine ethers. Guided by literature reports for triazolopyridine amines, initial efforts were focused on preparing and testing various arylalkyl ethers. The data presented in Table 1 suggested that an alkyl chain length of 2-3 bonds was optimal, and that substitution of the aryl ring and its incorporation into a bicyclic ring system was well tolerated. Polarity in the form of a basic heteroarene decreased activity. These observations, along with the knowledge that the C-8 chlorine substitution on the TZP was a metabolic liability, guided the design of second generation analogs toward more hydrophobic and ring constrained triazolopyridine ethers bearing a C-8 trifluoromethyl group, which are exemplified in Table 2. Ultimately, aryl-substituted cyclohexyl, cyclobutyl, and *trans*-cyclopropylmethyl ethers all displayed excellent $mGlu_2$ PAM activity with good metabolic stability. Halogen substitution of the pendent aryl group generally improved metabolic stability. The homochiral *trans*-cyclopropylmethyl ether (+)-**7m** (also referred to as BMT-133218) was selected as an attractive candidate for further characterization. It showed potent $mGlu_2$ PAM functional activity, high selectivity for modulation of $mGlu_2$ versus $mGlu_3$, and demonstrated potent binding to the allosteric site of $mGlu_2$ in a radioligand displacement assay. Furthermore, increasing concentrations of BMT-133218 displayed a left-shift for the EC_{50} of glutamate, which is fully consistent with PAM mode of action. While BMT-133218 did exhibit a low level of agonist activity in the absence of glutamate, a similar observation has been reported for other $mGlu_2$ PAMs, including JNJ-42153605.[22]

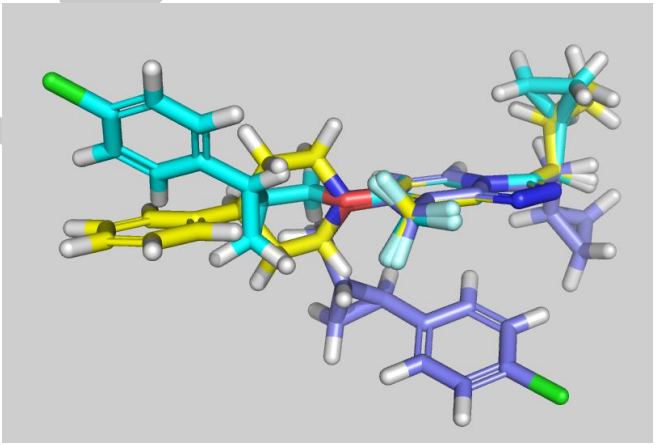

Figure 7. Computational modeling showing overlays of the global minimum for JNJ-42153605 (yellow), BMT-133218 (purple), and a low energy conformer (+ 2.7 kcal/mol) of BMT-133218 (blue).

With knowledge that BMT-133218 displayed good oral PK and micromolar brain drug levels at deliverable doses in rodents, this molecule was subjected to further characterization in multiple preclinical models relevant to positive and cognitive symptoms of schizophrenia. Toward this end, BMT-133218 reversed a PCP-stimulated increase in locomotion in mice at 10 mg/kg (*p.o.*). It also alleviated MK-801 induced cognitive deficits in both the two trial Y-maze performance in mice at 10 mg/kg (*p.o.*) and attentional set-shifting in rats in a dose dependent fashion at 3 and 10 mg/kg (*p.o.*). To our knowledge, this is the first report that an $mGlu_2$ PAM alleviates cognitive deficits in working memory and attention in acute NMDA antagonist models of CIAS. Reversal of cognitive impairment was also detected in a neonatal PCP model (unpublished observations), an effect not detected with $mGlu_2$ agonists. All together, these experiments suggest that the TZP ether BMT-133218 has potential utility to alleviate the positive symptoms and improve cognitive deficits of schizophrenia. For all experiments a rudimentary pharmacodynamic/pharmacokinetic relationship could be assembled using exposure data from satellite animals. This analysis suggests that free plasma drug

concentrations of at least 30 times the functional $mGlu_2$ EC_{50} of 1.4 nM were necessary to achieve *in vivo* activity. While this value seems high, several factors have to be taken into consideration. First, brain concentrations of BMT-133218 were typically less than half of the drug plasma concentrations. Secondly, protein binding data in plasma may not accurately reflect protein binding in brain tissue. Indeed, exploratory studies using rat brain homogenates suggested that BMT-133218 may be as much as 99.9% protein bound in brain tissue (data not shown). Lastly, exposure data used to calculate the free drug plasma levels for the *in vivo* experiments only came from a single time point at t = 1 h, and behavioral observations were often collected over a period of hours. Regardless of the analysis, it remains evident that high concentrations of BMT-133218 in plasma (≥ 3.8 μM at t = 1 h) were required to drive activity in preclinical models. The need for high active exposures of BMT-133218 created concern for the continued progression of this lead molecule. Areas for improvement included formulation/delivery of a poorly soluble compound, off-target activity, and drug-drug interactions. Extensive profiling and safety characterization of BMT-133218 revealed significant inhibition of the hERG ion channel (patch clamp hERG IC_{50} = 0.38 uM) and submicromolar inhibition of cytochrome P450 2C19 (rCYP2C19 IC_{50} = 0.62 uM). While the hERG liability could not be fully assessed without knowledge of unbound plasma concentrations at the projected human dose (an exercise that was not undertaken), the inhibition of CYP2C19 was a potential risk for drug-drug interactions. Many, if not all, of the known issues with BMT-133218, including extensive protein binding, inactivity at lower oral doses, poor solubility, hERG, and CYP inhibition were likely intertwined and a result of the highly lipophilic character of this molecule. It was our conclusion that improvements in the PK/PD relationship and reducing liabilities for TZP ethers must involve a reduction in lipophilicity. Not surprisingly, balancing lipophilicity and the $mGlu_2$ PAM activity of related small molecules has been a recognized challenge.[22]

In summary, the synthesis, *in vitro* $mGlu_2$ PAM activity, and metabolic stability data for a series of triazolopyridine (TZP) ether analogs was provided. The effort resulted in the discovery of a potent, selective, and brain penetrant lead molecule BMT-133218 ((+)-**7m**) with activity in several rodent models that recapitulate the symptoms and cognitive deficits of schizophrenia. Inactivity at lower doses was likely the result of high lipophilicity. Optimized triazolopyridine ethers may offer utility as $mGlu_2$ PAMs for the treatment of schizophrenia. Our continued efforts toward this end will be disclosed in due course.

6. Chemistry

Unless otherwise noted, all reagents and materials were obtained from commercial suppliers and used without further purification. Reactions involving air- or moisture-sensitive reagents were performed under a nitrogen or argon atmosphere. Silica gel chromatography was performed using prepacked silica gel cartridges (Biotage or ISCO). NMR spectra were recorded with Bruker spectrometers. Chemical shifts are reported in parts per million (ppm, d units). All final compounds were purified to 95% purity unless otherwise noted as determined by LCMS (LCAP at 215 nm) obtained on an Agilent 1100 or 1200 spectrometer using one of the following methods: Method A: column = XBridge C18, 19 x 200 mm, 5-μm particles; mobile phase A = 5:95 acetonitrile : water with 10-mM ammonium acetate; mobile phase B = 95/5 acetonitrile : water with 10-mM ammonium acetate; gradient = 30-70% B over 20 minutes, then a 7-minute hold at 100% B; flow = 20 mL/min. Standard conditions typically used for reverse phase preparative HPLC are as follows: column = Sunfire PrepC18 OBD 10 μm, 50 x 250 mm column; mobile phase A = 90% MeOH/10% water with 0.1% TFA; mobile phase B = 90% MeOH/10% water with 0.1% TFA; linear gradient 10-100 % B over 34 min, then a 20 minute hold at 100% B; flow = 50 mL/min. Low-resolution mass spectrometry (MS) data were obtained using ES ionization mode (positive).

6.1 General synthetic procedure for final products 9a-n

Examples **9 a-n** were prepared in parallel fashion according to the following method. A stock solution of 8-chloro-3-(cyclopropylmethyl)-7-iodo-[1,2,4]triazolo[4,3-a]pyridine[22] (0.9 M in toluene, 1 mL, 0.090 mmol) was added to a 2.0-5.0 mL microwave vial charged with the corresponding commercially available alcohol (0.648 mmol), cesium carbonate (50.0 mg, 0.153 mmol), 1,10-phenanthroline (20.0 mg, 0.111 mmol), and 20.0 mg of copper(I) iodide (20.0 mg, 0.105 mmol). The vials were sealed and heated to 100 °C for 17 hours. The reaction mixtures were cooled to rt, diluted with 0.5 mL of acetonitrile, and then filtered. The filtrates were concentrated in vacuo at 34 °C for 1 hour. Each sample was diluted with 0.5 mL of DMF (0.5 mL) and purified using reverse phase preparative LC-MS to afford the title product.

6.1.2 8-Chloro-7-(benzyloxy)-3-(cyclopropylmethyl)-[1,2,4]triazolo[4,3-a]pyridine (9a). 9% yield as a colorless oil; ^{1}H NMR (500MHz, METHANOL-d_4) δ ppm 8.49 (d, J=7.6 Hz, 1H), 7.54 - 7.50 (m, 2H), 7.46 - 7.41 (m, 2H), 7.40 - 7.36 (m, 2H), 5.49 (s, 2H), 3.09 (d, J=6.9 Hz, 2H), 1.33 - 1.24 (m, 1H), 0.69 - 0.64 (m, 2H), 0.39 - 0.35 (m, 2H); LC–MS $(M+H)^+$ 314.2.

6.1.3 8-chloro-7-((4-chlorobenzyl)oxy)-3-(cyclopropylmethyl)-[1,2,4]triazolo[4,3-a]pyridine (9b). 12% yield as a white solid; ^{1}H NMR (500MHz, METHANOL-d_4) δ 8.67 (d, *J*=7.6 Hz, 1H), 7.56 (d, *J*=7.6 Hz, 1H), 7.54 - 7.49 (m, 2H), 7.48 - 7.41 (m, 2H), 5.53 (s, 2H), 3.11 (d, *J*=6.9 Hz, 2H), 1.36 - 1.25 (m, 1H), 0.73 - 0.66 (m, 2H), 0.42 - 0.36 (m, 2H); LC–MS $(M+H)^+$ 348.4.

6.1.4 8-chloro-7-((3-chlorobenzyl)oxy)-3-(cyclopropylmethyl)-[1,2,4]triazolo[4,3-a]pyridine (9c). 31% yield as a colorless oil; ^{1}H NMR (500 MHz, DMSO-d_6) δ 8.51 (d, *J*=7.6 Hz, 1H), 7.58 (s, 1H), 7.52 - 7.39 (m, 3H), 7.23 (d, *J*=7.6 Hz, 1H), 5.46 (s, 2H), 3.04 (d, *J*=7.0 Hz, 2H), 1.19 (s, 1H), 0.62 - 0.45 (m, 2H), 0.28 (d, *J*=5.2 Hz, 2H); LC–MS $(M+H)^+$ 348.1.

6.1.5 8-chloro-7-((2-chlorobenzyl)oxy)-3-(cyclopropylmethyl)-[1,2,4]triazolo[4,3-a]pyridine (9d). 19% yield as a colorless oil; ^{1}H NMR (500 MHz, DMSO-d_6) δ 8.53 (d, *J*=7.6 Hz, 1H), 7.71 - 7.64 (m, 1H), 7.60 - 7.53 (m, 1H), 7.48 - 7.40 (m, 2H), 7.29 (d, *J*=7.6 Hz, 1H), 5.48 (s, 2H), 3.05 (d, *J*=7.0 Hz, 2H), 1.26 - 1.13 (m, 1H), 0.56 - 0.48 (m, 2H), 0.32 - 0.25 (m, 2H); LC–MS $(M+H)^+$ 348.4.

6.1.6 7-([1,1'-biphenyl]-4-ylmethoxy)-8-chloro-3-(cyclopropylmethyl)-[1,2,4]triazolo[4,3-a]pyridine (9e). 22% yield as a colorless oil; ^{1}H NMR (500MHz, DMSO-d_6) δ 8.50 (d, *J*=7.6 Hz, 1H), 7.76 - 7.67 (m, 4H), 7.59 (d, *J*=7.9 Hz, 2H), 7.48 (t, *J*=7.6 Hz, 2H), 7.42 - 7.36 (m, 1H), 7.28 (d, *J*=7.6 Hz, 1H), 5.50 (s, 2H), 3.04 (d, *J*=7.0 Hz, 2H), 1.19 (br. s., 1H), 0.55 - 0.48 (m, 2H), 0.28 (q, *J*=4.8 Hz, 2H); LC–MS $(M+H)^+$ 390.4.

6.1.7 7-([1,1'-biphenyl]-3-ylmethoxy)-8-chloro-3-(cyclopropylmethyl)-[1,2,4]triazolo[4,3-a]pyridine (9f). 20% yield as a colorless oil; ^{1}H NMR (500MHz, DMSO-d_6) δ 8.55 - 8.38 (m, 1H), 7.77 - 7.59 (m, 3H), 7.59 - 7.44 (m, 5H), 7.39 (br. s., 1H), 7.33 - 7.24 (m, 1H), 5.51 (br. s., 2H), 3.06 - 2.93 (m, 2H),

1.16 (br. s., 1H), 0.50 (d, *J*=5.2 Hz, 2H), 0.26 (br. s., 2H); LC–MS $(M+H)^+$ 390.4.

6.1.8 7-([1,1'-biphenyl]-2-ylmethoxy)-8-chloro-3-(cyclopropylmethyl)-[1,2,4]triazolo[4,3-a]pyridine (9g). 41% yield as a colorless oil; ^{1}H NMR (500MHz, DMSO-d_6) δ 8.42 (d, *J*=7.3 Hz, 1H), 7.66 (d, *J*=7.0 Hz, 1H), 7.50 - 7.36 (m, 8H), 7.00 (d, *J*=7.3 Hz, 1H), 5.23 (s, 2H), 3.00 (br. s., 2H), 1.16 (br. s., 1H), 0.50 (d, *J*=7.3 Hz, 2H), 0.26 (br. s., 2H); LC–MS $(M+H)^+$ 390.4.

6.1.9 8-chloro-3-(cyclopropylmethyl)-7-(naphthalen-2-ylmethoxy)-[1,2,4]triazolo[4,3-a]pyridine (9h). 17% yield as a colorless oil; ^{1}H NMR (500MHz, DMSO-d_6) δ 8.49 (d, *J*=7.6 Hz, 1H), 8.02 - 7.93 (m, 4H), 7.63 (dd, *J*=8.4, 1.7 Hz, 1H), 7.57 - 7.53 (m, 2H), 7.30 (d, *J*=7.6 Hz, 1H), 5.62 (s, 2H), 3.02 (d, *J*=6.7 Hz, 2H), 1.20 - 1.14 (m, 1H), 0.53 - 0.48 (m, 2H), 0.30 - 0.24 (m, 2H); LC–MS $(M+H)^+$ 364.2.

6.1.10 8-chloro-3-(cyclopropylmethyl)-7-((1,2,3,4-tetrahydronaphthalen-2-yl)oxy)-[1,2,4]triazolo[4,3-a]pyridine (9i). 3% yield as a colorless oil; ^{1}H NMR (500MHz, METHANOL-d_4) δ 8.37 (d, *J*=7.3 Hz, 1H), 7.24 (d, *J*=7.6 Hz, 1H), 7.15 - 7.05 (m, 4H), 5.13 (br. s., 1H), 3.26 (dd, *J*=16.5, 4.6 Hz, 1H), 3.16 - 3.01 (m, 4H), 2.95 - 2.84 (m, 1H), 2.25 - 2.10 (m, 2H), 1.32 - 1.22 (m, 1H), 0.69 - 0.59 (m, 2H), 0.40 - 0.31 (m, 2H); LC–MS $(M+H)^+$ 354.3.

6.1.11 8-chloro-3-(cyclopropylmethyl)-7-(pyridin-3-ylmethoxy)-[1,2,4]triazolo[4,3-a]pyridine (9j). 6% yield as a colorless oil; ^{1}H NMR (500MHz, METHANOL-d_4) δ 8.80 (s, 1H), 8.64 (d, *J*=4.3 Hz, 1H), 8.53 (d, *J*=7.8 Hz, 1H), 8.18 (d, *J*=8.1 Hz, 1H), 7.65 (dd, *J*=8.1, 5.3 Hz, 1H), 7.41 (d, *J*=7.6 Hz, 1H), 5.57 (s, 2H), 3.11 (d, *J*=7.0 Hz, 2H), 1.29 (dd, *J*=11.7, 4.8 Hz, 1H), 0.69 - 0.64 (m, 2H), 0.40 - 0.36 (m, 2H); LC–MS $(M+H)^+$ 315.2.

6.1.12 8-chloro-3-(cyclopropylmethyl)-7-(pyridin-2-ylmethoxy)-[1,2,4]triazolo[4,3-a]pyridine (9k). 62% yield as a colorless oil; ^{1}H NMR (500MHz, DMSO-d_6) δ 8.52 (d, *J*=7.3 Hz, 1H), 7.37 - 7.22 (m, 6H), 5.37 (s, 2H), 3.04 (d, *J*=6.7 Hz, 2H), 1.18 (d, *J*=6.7 Hz, 1H), 0.54 - 0.49 (m, 2H), 0.28 (q, *J*=5.0 Hz, 2H); LC–MS $(M+H)^+$ 315.2.

6.1.13 8-chloro-3-(cyclopropylmethyl)-7-((3-(pyrimidin-5-yl)benzyl)oxy)-[1,2,4]triazolo[4,3-a]pyridine (9l). 7% yield as a colorless oil; ^{1}H NMR (500MHz, DMSO-d_6) δ 9.20 (br. s., 1H), 9.16 - 9.11 (m, 2H), 8.46 (s, 1H), 7.92 (br. s., 1H), 7.80 (br. s., 1H), 7.60 (br. s., 3H), 5.50 (br. s., 2H), 3.00 (br. s., 2H), 1.16 (br. s., 1H), 0.49 (br. s., 2H), 0.25 (br. s., 2H); LC–MS $(M+H)^+$ 392.4.

6.1.14 8-(((8-chloro-3-(cyclopropylmethyl)-[1,2,4]triazolo[4,3-a]pyridin-7-yl)oxy)methyl)isoquinoline (9m). 6% yield as a colorless oil; ^{1}H NMR (500MHz, DMSO-d_6) δ 8.42 (d, *J*=7.3 Hz, 1H), 7.66 (d, *J*=7.0 Hz, 1H), 7.47 - 7.38 (m, 5H), 7.00 (d, *J*=7.3 Hz, 1H), 5.23 (s, 2H), 3.00 (br. s., 2H), 1.16 (br. s., 1H), 0.50 (d, *J*=7.3 Hz, 2H), 0.26 (br. s., 2H); LC–MS $(M+H)^+$ 365.4.

6.1.15 8-chloro-3-(cyclopropylmethyl)-7-phenethoxy-[1,2,4]triazolo[4,3-a]pyridine (9n). 24% yield as a colorless oil; ^{1}H NMR (500 MHz, DMSO-d_6) δ 8.47 (d, *J*=7.6 Hz, 1H), 7.41 - 7.31 (m, 4H), 7.28 - 7.22 (m, 1H), 7.19 (d, *J*=7.6 Hz, 1H), 4.49 (t, *J*=6.9 Hz, 2H), 3.10 (t, *J*=6.9 Hz, 2H), 3.04 (d, *J*=7.0 Hz, 2H), 1.23 - 1.12 (m, 1H), 0.54 - 0.48 (m, 2H), 0.30 - 0.24 (m, 2H); LC–MS $(M+H)^+$ 328.2.

6.2 7-(benzyloxy)-3-(cyclopropylmethyl)-8-(trifluoromethyl)-[1,2,4]triazolo[4,3-a]pyridine (7a)

6.2.1. (4-(benzyloxy)-2-chloro-3-(trifluoromethyl)pyridine. A solution of benzyl alcohol (commercially available, 1.201 mL, 11.55 mmol) was added to a mixture of 60% sodium hydride dispersion in mineral oil (0.484 g, 12.10 mmol) and DMF (30 mL) in an ice bath at 0 °C. The mixture was allowed to stir at 0 °C for 30 min, then a solution of 2,4-dichloro-3-(trifluoromethyl)pyridine[30] (2.376 g, 11 mmol) in DMF (3 mL) was quickly added. The resulting mixture was stirred at 0 °C for 1 hour, then quenched by the addition of water. The aqueous mixture was extracted with ethyl acetate. The combined organic layers were washed with brine, dried over magnesium sulfate, filtered, and concentrated in vacuo. The residue was purified using silica gel column chromatography (5:1 hexanes/ethyl acetate) to afford 4-(benzyloxy)-2-chloro-3-(trifluoromethyl)pyridine (1.59 g, 50 % yield) as a white solid. ^{1}H NMR (400MHz, $CDCl_3$) δ 8.36 (d, *J*=5.9 Hz, 1H), 7.47 - 7.37 (m, 6H), 6.95 (d, *J*=5.6 Hz, 1H), 5.28 (s, 2H); LC–MS $(M+H)^+$ 288.1. $CDCl_3$

6.2.2. 4-(benzyloxy)-2-hydrazinyl-3-(trifluoromethyl)pyridine. A mixture of 4-(benzyloxy)-2-chloro-3-(trifluoromethyl)pyridine (from step 6.2.1, 1.2 g, 4.17 mmol), dioxane (10 mL), and hydrazine monohydrate (4.08 mL, 83 mmol) was heated together in a sealed vial for 18 h in an oil bath at 100 °C. The reaction mixture was cooled to rt and concentrated in vacuo. The residue was partitioned between aqueous sodium bicarbonate and dichloromethane. The aqueous layer was extracted with dichloromethane. The combined organic extracts were washed with brine, dried over magnesium sulfate, filtered, and concentrated in vacuo to afford 4-(benzyloxy)-2-hydrazinyl-3-(trifluoromethyl)pyridine (820 mg, 69 % yield) as an off-white solid. LC–MS (M+H)+ 284.1.

6.2.3. N'-(4-(benzyloxy)-3-(trifluoromethyl)pyridin-2-yl)-2-cyclopropylacetohydrazide. A 1.0 M solution of 2-cyclopropylacetyl chloride in DCM (3.99 mL, 3.99 mmol) was added to a flask charged with a solution of 4-(benzyloxy)-2-hydrazinyl-3-(trifluoromethyl)pyridine (from step 6.2.2., 946 mg, 3.34 mmol) and triethylamine (0.70 mL, 5.01 mmol) in DCM (30 mL) at 0 °C. After 1 h at 0 °C, the reaction was diluted with water. The aqueous mixture was extracted with DCM. The organic extracts were washed with brine, dried (sodium sulfate), filtered, and concentrated in vacuo to afford N'-(4-(benzyloxy)-3-(trifluoromethyl)pyridin-2-yl)-2-cyclopropylacetohydrazide (943 mg, 77% yield). The crude product was carried forward without purification. ^{1}H NMR (500MHz, $CDCl_3$) δ 8.13 (d, *J*=5.8 Hz, 1H), 7.43 - 7.40 (m, 5H), 6.49 (d, *J*=5.6 Hz, 1H), 5.22 (s, 2H), 2.30 (d, *J*=7.2 Hz, 2H), 1.15 - 1.08 (m, 1H), 0.70 - 0.65 (m, 2H), 0.32 - 0.27 (m, 2H); LC–MS $(M+H)^+$ 366.2.

6.2.4 7-(benzyloxy)-3-(cyclopropylmethyl)-8-(trifluoromethyl)-[1,2,4]triazolo[4,3-a]pyridine. A mixture of N'-(4-(benzyloxy)-3-(trifluoromethyl)pyridin-2-yl)-2-cyclopropylacetohydrazide (from step 6.2.3, 20 mg, 0.55 mmol), Burgess reagent (26.1 mg, 0.109 mmol), acetonitrile (2 mL), and dioxane (2 mL) was heated at 85 °C in a sealed vial for 18 h. After cooling to rt, the reaction mixture was evaporated in vacuo and the residue was partitioned between water and ethyl acetate. The aqueous layer was extracted with ethyl acetate, and the combined organic layers were washed with brine, dried over magnesium sulfate, filtered and concentrated in vacuo. The crude product was dissolved in a minimum amount of boiling ethyl acetate. The solution was allowed to cool to rt. After 3 h, the crystalline solid was collected by vacuum filtration to afford 7-(benzyloxy)-3-(cyclopropylmethyl)-8-(trifluoromethyl)-[1,2,4]triazolo[4,3-a]pyridine (19 mg, 95 % yield) as a white solid. ^{1}H NMR (400MHz, METHANOL-d_4) δ 8.97 (d, *J*=7.8

Hz, 1H), 7.75 (d, *J*=7.8 Hz, 1H), 7.55 - 7.51 (m, 2H), 7.49 - 7.38 (m, 3H), 5.66 (s, 2H), 3.14 (d, *J*=6.8 Hz, 2H), 1.37 - 1.27 (m, 1H), 0.77 - 0.66 (m, 2H), 0.42 (q, *J*=4.9 Hz, 2H); LC–MS $(M+H)^+$ 348.2.

6.3 3-(cyclopropylmethyl)-7-(2,2-difluoro-2-phenylethoxy)-8-(trifluoromethyl)-[1,2,4]triazolo[4,3-a]pyridine (7b)

6.3.1. 2,2-difluoro-2-phenylethanol. To a stirring suspension of LAH (0.265 g, 6.98 mmol) in THF (3.0 mL) was added dropwise a solution of ethyl 2,2-difluoro-2-phenylacetate (commercial, 345 mg, 1.72 mmol) in THF (2.0 mL). The resulting mixture was stirred at rt for 18 h. The reaction was quenched by the addition of aqueous ammonium hydroxide solution. The reaction mixture was slurried in a bilayer of water and ethyl acetate and filtered through celite. The layers were separated and the aqueous layer was extracted with ethyl acetate. The combined organic layers were washed with brine, dried (magnesium sulfate), filtered, and concentrated in vacuo. The residue was purified by silica-gel column chromatography (10-15% ethyl acetate/hexane) to afford (2,2-difluoro-2-phenylethanol (180 mg, 66% yield). ^{1}H NMR (400 MHz, $CDCl_3$) δ 7.58 - 7.36 (m, 5H), 3.98 (td, J=13.4, 6.0 Hz, 2H), 2.14 (t, J=6.4 Hz, 1H).

6.3.2. 2-chloro-4-(2,2-difluoro-2-phenylethoxy)-3-(trifluoromethyl)pyridine. This material was prepared from 6.3.1. and 2,4-dichloro-3-(trifluoromethyl)pyridine[32] according to the procedure described in step 6.2.1. to afford 2-chloro-4-(2,2-difluoro-2-phenylethoxy)-3-(trifluoromethyl)pyridine (221 mg, 58% yield) as an orange oil. ^{1}H NMR (500MHz, $CDCl_3$) δ 8.37 (d, *J*=5.8 Hz, 1H), 7.60 - 7.56 (m, 2H), 7.49 (q, *J*=7.1 Hz, 3H), 6.85 (d, *J*=5.8 Hz, 1H), 4.49 (t, *J*=11.1 Hz, 2H).

6.3.3. 4-(2,2-Difluoro-2-phenylethoxy)-2-hydrazinyl-3-(trifluoromethyl)pyridine. 4-(2,2-Difluoro-2-phenylethoxy)-2-hydrazinyl-3-(trifluoromethyl)pyridine (186 mg, 86 % yield) was prepared from 2-chloro-4-(2,2-difluoro-2-phenylethoxy)-3-(trifluoromethyl)pyridine (from step 6.3.2) following a procedure analogous to step 6.2.2. ^{1}H NMR (500 MHz, $CDCl_3$) δ 8.23 - 8.12 (m, 1H), 7.62 - 7.43 (m, 5H), 6.54 (br s, 1H), 6.28 (d, *J*=6.0 Hz, 1H), 4.43 (t, *J*=11.1 Hz, 2H), 3.99 (t, *J*=13.4 Hz, 2H).

6.3.4. 3-(Cyclopropylmethyl)-7-(2,2-difluoro-2-phenylethoxy)-8-(trifluoromethyl)-[1,2,4]triazolo[4,3-a]pyridine. The titled compound (59 mg, 17 % yield over 2 steps) was prepared from 4-(2,2-difluoro-2-phenylethoxy)-2-hydrazinyl-3-(trifluoromethyl)pyridine (from preparation 6.3.3.) following procedures analogous to steps 6.2.3 and 6.2.4. The final product was purified by silica gel column chromatography (100 % ethyl acetate) and reverse phase preparatory HPLC. ^{1}H NMR (500 MHz, METHANOL-d_4) δ 8.56 (d, *J*=7.8 Hz, 1H), 7.65 (dd, *J*=7.6, 1.8 Hz, 2H), 7.56 - 7.47 (m, 3H), 7.19 (d, *J*=7.8 Hz, 1H), 3.08 (d, *J*=6.9 Hz, 2H), 1.29 - 1.17 (m, 1H), 0.63 (dd, *J*=8.1, 1.4 Hz, 2H), 0.42 - 0.31 (m, 2H); LC–MS $(M+H)^+$ 398.2.

6.4 3-(cyclopropylmethyl)-7-(2-(4-fluorophenyl)propoxy)-8-(trifluoromethyl)-[1,2,4]triazolo[4,3-a]pyridine, TFA salt (7c)

6.4.1. (2-fluoro-2-phenylethanol. 2,2-difluoro-2-phenylethanol (371 mg, 73 % yield) was prepared from methyl 2-fluoro-2-phenylacetate (commercially available) following a procedure analogous to step 6.3.1. ^{1}H NMR (500 MHz, $CDCl_3$) δ 7.45 - 7.24 (m, 1H), 5.65 - 5.51 (m, 1H), 4.01 - 3.78 (m, 3H), 2.26 (dd, *J*=8.4, 4.6 Hz, 1H).

6.4.2. 3-(cyclopropylmethyl)-7-(2-(4-fluorophenyl)propoxy)-8-(trifluoromethyl)-[1,2,4]triazolo[4,3-a]pyridine. A solution of 2-(4-fluorophenyl)propan-1-ol (from step 6.4.1., 69.9 mg, 0.453 mmol) in toluene (0.5 mL) was added to a microwave vial charged with 7-chloro-3-(cyclopropylmethyl)-8-(trifluoromethyl)-[1,2,4]triazolo[4,3-a]pyridine (**18**)[22] (25 mg, 0.091 mmol, cesium carbonate (59.1 mg, 0.181 mmol), (*S*)-(*R*)-JOSIPHOS (11 mg, 0.018 mmol), and allylpalladium chloride dimer (3.3 mg, 9.1 µmol). The vessel was flushed with nitrogen then sealed with a teflon coated cap. The mixture was heated at 135 °C for 2 h. The reaction was cooled to rt. The crude reaction mixture was purified by silica gel column chromatography (100% EtOAc) and was further purified using reverse phase preparatory HPLC to afford the title compound (9.4 mg, 20% yield) as a TFA salt. ^{1}H NMR (500 MHz, METHANOL-d_4) δ 8.52 (d, J=7.8 Hz, 1H), 7.44 - 7.28 (m, 2H), 7.14 (d, J=7.9 Hz, 1H), 7.10 - 6.98 (m, 2H), 4.49 - 4.29 (m, 2H), 3.40 - 3.20 (m, 1H), 3.05 (d, J=6.9 Hz, 2H), 1.44 (d, J=7.0 Hz, 3H), 1.27 - 1.14 (m, 1H), 0.67 - 0.53 (m, 2H), 0.40 - 0.26 (m, 2H); LC–MS $(M+H)^+$ 394.1.

6.5 3-(cyclopropylmethyl)-7-(2-(4-fluorophenyl)-2-methylpropoxy)-8-(trifluoromethyl)-[1,2,4]triazolo[4,3-a]pyridine (7d)

6.5.1. 2-(4-fluorophenyl)-2-methylpropanenitrile. A solution of 1.0 M potassium *tert*-butoxide in *tert*-butanol (92 mL, 92 mmol) was added to a mixture of 2-(4-fluorophenyl)acetonitrile (commercially available, 5.0 g, 37.0 mmol), iodomethane (6.36 mL, 102 mmol), and THF (100 mL) maintained at 0 °C. After complete addition, the cold bath was removed and the mixture was allowed to stir at rt for 18 h. The reaction was quenched with a saturated aqueous solution of ammonium chloride, poured into water, and extracted with ethyl acetate. The combined organics were washed with brine, dried (magnesium sulfate), filtered, and concentrated in vacuo. The crude product was purified using silica gel column chromatography (40:1 hexane/ethyl acetate) to afford 2-(4-fluorophenyl)-2-methylpropanenitrile (5.2 g, 84 % yield) as a clear liquid. ^{1}H NMR (500 MHz, $CDCl_3$) δ 7.50 - 7.41 (m, 2H), 7.14 - 7.03 (m, 2H), 1.73 (s, 6H).

6.5.2. 2-(4-fluorophenyl)-2-methylpropanoic acid. A mixture of 2-(4-fluorophenyl)-2-methylpropanenitrile (from step 6.5.1., 5.2 g, 31.9 mmol) and 15% aqueous sodium hydroxide (80 mL) was heated at reflux for 16 h. The mixture was cooled to rt and extracted with diethyl ether. The aqueous layer was made acidic with 1 N aqueous hydrochloric acid (300 mL) and was then extracted with diethyl ether. The acidic organic extract was washed with brine, dried (magnesium sulfate), filtered and concentrated in vacuo. The residue was dried under high vacuum for several hours to afford 2-(4-fluorophenyl)-2-methylpropanoic acid (1.89 g, 33 % yield) as a white solid. ^{1}H NMR (500 MHz, $CDCl_3$) δ 7.44 - 7.32 (m, 2H), 7.09 - 6.97 (m, 2H), 1.60 (s, 6H).

6.5.3. 2-(4-Fluorophenyl)-2-methylpropan-1-ol. 2-(4-fluorophenyl)-2-methylpropan-1-ol (1.77 g, quantitative yield) was prepared from 2-(4-fluorophenyl)-2-methylpropanoic acid (from step 6.5.2.) following a procedure analogous to step 6.3.1. ^{1}H NMR (500 MHz, $CDCl_3$) δ 7.42 - 7.32 (m, 2H), 7.08 - 6.98 (m, 2H), 3.61 (s, 2H), 1.34 (s, 6H).

6.5.4. 3-(cyclopropylmethyl)-7-(2-(4-fluorophenyl)-2-methylpropoxy)-8-(trifluoromethyl)-[1,2,4]triazolo[4,3-a]pyridine. The titled compound (13 mg, 13 % yield) was prepared from 2-(4-fluorophenyl)-2-methylpropan-1-ol (6.5.3.) and 7-chloro-3-(cyclopropylmethyl)-8-(trifluoromethyl)-[1,2,4]triazolo[4,3-a]pyridine (**18**)[22] following the procedure analogous to example 6.4.2. The final product was purified using preparative LC/MS (column: XBridge C18, 19 x mm, 5-µm particles; mobile phase A: 5:95 acetonitrile/water with 10-mM

ammonium acetate; mobile phase B: 95:5 acetonitrile/water with 10-mM ammonium acetate; gradient: 30-70% B over 15 minutes, then a 7-minute hold at 100% B; flow: 20 mL/min). ^{1}H NMR (500 MHz, DMSO-d_6) δ 8.66 (d, J=7.6 Hz, 1H), 7.50 (dd, J=8.5, 5.5 Hz, 2H), 7.23 - 7.07 (m, 3H), 4.33 (s, 2H), 3.02 (d, J=7.0 Hz, 2H), 1.40 (s, 6H), 1.15 (br. s., 1H), 0.49 (d, J=6.4 Hz, 2H), 0.25 (d, J=4.0 Hz, 2H); LC–MS $(M+H)^+$ 408.2.

6.6 7-(2-(4-chlorophenyl)-2-methylpropoxy)-3-(cyclopropylmethyl)-8-(trifluoromethyl)-[1,2,4]triazolo[4,3-a]pyridine (7e)

6.6.1. 2-chloro-4-(2-(4-chlorophenyl)-2-methylpropoxy)-3-(trifluoromethyl)pyridine. 2-chloro-4-(2-(4-chlorophenyl)-2-methylpropoxy)-3-(trifluoromethyl)pyridine (810 mg, 82 % yield) was prepared from 2-(4-chlorophenyl)-2-methylpropan-1-ol (commercially available) and 2,4-dichloro-3-(trifluoromethyl)pyridine[32] following a procedure analogous to step 6.2.1. LC–MS $(M+H)^+$ 363.9. ^{1}H NMR (500 MHz, $CDCl_3$) δ 8.32 (d, *J*=5.8 Hz, 1H), 7.39 - 7.29 (m, 4H), 6.82 (d, *J*=5.8 Hz, 1H), 4.00 (s, 2H), 1.49 (s, 6H).

6.6.2. 4-(2-(4-chlorophenyl)-2-methylpropoxy)-2-hydrazinyl-3-(trifluoromethyl)pyridine. 4-(2-(4-chlorophenyl)-2-methylpropoxy)-2-hydrazinyl-3-(trifluoromethyl)pyridine (457 mg, quantitative yield) was prepared from 2-chloro-4-(2-(4-chlorophenyl)-2-methylpropoxy)-3-(trifluoromethyl)pyridine (from step 6.6.1.) following a procedure analogous to step 6.2.2. ^{1}H NMR (500 MHz, DMSO-d_6) δ 8.16 (d, *J*=5.8 Hz, 1H), 7.52 - 7.41 (m, 2H), 7.41 - 7.30 (m, 3H), 6.55 (d, *J*=6.0 Hz, 1H), 4.26 (s, 2H), 4.11 (s, 2H), 1.37 (s, 6H); LC–MS $(M+H)^+$ 360.1.

6.6.3. 7-(2-(4-chlorophenyl)-2-methylpropoxy)-3-(cyclopropylmethyl)-8-(trifluoromethyl)-[1,2,4]triazolo[4,3-a]pyridine. The titled compound (157 mg, 65 % yield over 2 steps) was prepared from 4-(2-(4-chlorophenyl)-2-methylpropoxy)-2-hydrazinyl-3-(trifluoromethyl)pyridine (from step 6.6.2., 200 mg, 0.556 mmol) following procedures analogous to steps 6.2.3. and 6.2.4. The final product was purified by silica gel column chromatography (100% EtOAc). ^{1}H NMR (500 MHz, $CDCl_3$) δ 8.06 (d, *J*=7.6 Hz, 1H), 7.46 - 7.36 (m, 2H), 7.36 - 7.29 (m, 2H), 6.72 (d, *J*=7.8 Hz, 1H), 4.10 (s, 2H), 3.06 (d, *J*=6.7 Hz, 2H), 1.53 (s, 6H), 1.21 - 1.08 (m, 1H), 0.70 - 0.55 (m, 2H), 0.32 (q, *J*=5.0 Hz, 2H); LC–MS $(M+H)^+$ 424.2.

6.7 3-(cyclopropylmethyl)-7-((1-(4-fluorophenyl)cyclopropyl)methoxy)-8-(trifluoromethyl)-[1,2,4]triazolo[4,3-a]pyridine (7f)

6.7.1. 2-chloro-4-((1-(4-fluorophenyl)cyclopropyl)methoxy)-3-(trifluoromethyl)pyridine. 2-chloro-4-((1-(4-fluorophenyl)cyclopropyl)methoxy)-3-(trifluoromethyl)pyridine (537 mg, 86 % yield) was prepared from (1-(4-fluorophenyl)cyclopropyl)methanol (commercially available) and 2,4-dichloro-3-(trifluoromethyl)pyridine[32] following a procedure analogous to step 6.2.1. ^{1}H NMR (500 MHz, $CDCl_3$) δ 8.30 (d, *J*=6.0 Hz, 1H), 7.43 - 7.38 (m, 2H), 7.04 - 6.98 (m, 2H), 6.75 (d, *J*=5.8 Hz, 1H), 4.10 (s, 2H), 1.08 - 1.00 (m, 4H); LC–MS $(M+H)^+$ 346.0.

6.7.2. 4-((1-(4-fluorophenyl)cyclopropyl)methoxy)-2-hydrazinyl-3-(trifluoromethyl)pyridine. 4-((1-(4-fluorophenyl)cyclopropyl)methoxy)-2-hydrazinyl-3-(trifluoromethyl)pyridine (500 mg, 94 % yield) was prepared from 2-chloro-4-((1-(4-fluorophenyl)cyclopropyl)methoxy)-3-(trifluoromethyl)pyridine (from step 6.7.1.) following a procedure analogous to step 6.2.2 (b). LC–MS $(M+H)^+$ 342.0.

6.7.3. 3-(cyclopropylmethyl)-7-((1-(4-fluorophenyl)cyclopropyl)methoxy)-8-(trifluoromethyl)-[1,2,4]triazolo[4,3-a]pyridine. The titled compound (64 mg, 9 % yield over 2 steps) was prepared from 4-((1-(4-fluorophenyl)cyclopropyl)methoxy)-2-hydrazinyl-3-(trifluoromethyl)pyridine (from step 6.7.2.) following the procedures detailed in steps 6.2.3. and 6.2.4. The final product was purified by silica-gel column chromatography (0-100% ethyl acetate/hexanes). ^{1}H NMR (500 MHz, $CDCl_3$) δ 8.38 (d, *J*=7.6 Hz, 1H), 7.46 - 7.40 (m, 2H), 7.04 - 6.98 (m, 2H), 6.87 (d, *J*=7.8 Hz, 1H), 4.27 (s, 2H), 3.11 (d, *J*=6.7 Hz, 2H), 1.16 (br. s., 1H), 1.10 - 1.02 (m, 4H), 0.64 - 0.59 (m, 2H), 0.36 - 0.31 (m, 2H); LC–MS $(M+H)^+$ 405.8.

6.8 7-((1-(4-chlorophenyl)cyclopropyl)methoxy)-3-(cyclopropylmethyl)-8-(trifluoromethyl)-[1,2,4]triazolo[4,3-a]pyridine (7g)

6.8.1. 2-chloro-4-((1-(4-chlorophenyl)cyclopropyl)methoxy)-3-(trifluoromethyl)pyridine. 2-chloro-4-((1-(4-chlorophenyl)cyclopropyl)methoxy)-3-(trifluoromethyl)pyridine (438 mg, 74 % yield) was prepared from (1-(4-chlorophenyl)cyclopropyl)methanol (commercially available) and 2,4-dichloro-3-(trifluoromethyl)pyridine[32] following a procedure analogous to step 6.2.1. ^{1}H NMR (500 MHz, $CDCl_3$) δ 8.31 (d, *J*=5.8 Hz, 1H), 7.39 - 7.35 (m, 2H), 7.32 - 7.29 (m, 2H), 6.75 (d, *J*=6.0 Hz, 1H), 4.11 (s, 2H), 1.09 - 1.02 (m, 4H); LC–MS $(M+H)^+$ 362.0.

6.8.2. 4-((1-(4-Chlorophenyl)cyclopropyl)methoxy)-2-hydrazinyl-3-(trifluoromethyl)pyridine. 4-((1-(4-chlorophenyl)cyclopropyl)methoxy)-2-hydrazinyl-3-(trifluoromethyl)pyridine (439 mg, quantitative yield) was prepared from 2-chloro-4-((1-(4-chlorophenyl)cyclopropyl)methoxy)-3-(trifluoromethyl)pyridine (from step 6.8.1.) following a procedure analogous to step 6.2.2. LC–MS $(M+H)^+$ 358.0.

6.8.3. 7-((1-(4-chlorophenyl)cyclopropyl)methoxy)-3-(cyclopropylmethyl)-8-(trifluoromethyl)-[1,2,4]triazolo[4,3-a]pyridine. The titled compound (131 mg, 20 % yield over 2 steps) was prepared from 4-((1-(4-chlorophenyl)cyclopropyl)methoxy)-2-hydrazinyl-3-(trifluoromethyl)pyridine (from 6.8.2.) following procedures analogous to steps 6.2.3. and 6.2.4. The final product was purified by silica-gel column chromatography (100% ethyl acetate). ^{1}H NMR (500 MHz, $CDCl_3$) δ 8.23 (d, *J*=7.6 Hz, 1H), 7.46 - 7.40 (m, 2H), 7.04 - 6.97 (m, 2H), 6.77 (d, *J*=7.8 Hz, 1H), 4.25 (s, 2H), 3.09 (d, *J*=6.7 Hz, 2H), 1.19 - 1.12 (m, 1H), 1.10 - 1.02 (m, 4H), 0.65 - 0.59 (m, 2H), 0.35 - 0.30 (m, 2H); LC–MS $(M+H)^+$ 422.0.

6.9 3-(cyclopropylmethyl)-7-((1-phenylcyclohexyl)methoxy)-8-(trifluoromethyl)-[1,2,4]triazolo[4,3-a]pyridine (7h)

6.9.1. 2-chloro-4-((1-phenylcyclohexyl)methoxy)-3-(trifluoromethyl)pyridine. 2-chloro-4-((1-phenylcyclohexyl)methoxy)-3-(trifluoromethyl)pyridine (875 mg, 90 % yield) was prepared from (1-phenylcyclohexyl)methanol (commercially available) and 2,4-dichloro-3-(trifluoromethyl)pyridine[32] following a procedure analogous to step 6.2.1. ^{1}H NMR (500 MHz, $CDCl_3$) δ ppm 8.25 (d, J=6.0 Hz, 1H), 7.53 - 7.42 (m, 2H), 7.42 - 7.33 (m, 2H), 7.27 - 7.22 (m, 1H), 6.73 (d, J=6.0 Hz, 1H), 3.91 (s, 2H), 2.30 (d, J=13.3 Hz, 2H), 1.90 - 1.77 (m, 2H), 1.68 - 1.57 (m, 3H), 1.48 - 1.35 (m, 3H); LC–MS $(M+H)^+$ 370.0.

6.9.2. 2-hydrazinyl-4-((1-phenylcyclohexyl)methoxy)-3-(trifluoromethyl)pyridine. 2-hydrazinyl-4-((1-

phenylcyclohexyl)methoxy)-3-(trifluoromethyl)pyridine (437 mg, 92 % yield) was prepared from 2-chloro-4-((1-phenylcyclohexyl)methoxy)-3-(trifluoromethyl)pyridine (from step 6.9.1.) following a procedure analogous to step 6.2.2. ^{1}H NMR (500 MHz, DMSO-d_6) δ 8.10 (d, *J*=5.8 Hz, 1H), 7.44 (d, *J*=7.5 Hz, 2H), 7.33 (t, *J*=7.7 Hz, 3H), 7.24 - 7.12 (m, 1H), 6.46 (d, *J*=6.0 Hz, 1H), 4.25 (s, 2H), 3.96 (s, 2H), 2.19 (d, *J*=13.7 Hz, 2H), 1.84 - 1.69 (m, 2H), 1.62 - 1.41 (m, 3H), 1.39 - 1.20 (m, 3H); LC–MS $(M+H)^+$ 366.1.

6.9.3. 3-(cyclopropylmethyl)-7-((1-phenylcyclohexyl)methoxy)-8-(trifluoromethyl)-[1,2,4]triazolo[4,3-a]pyridine. The titled compound (107 mg, 45 % yield over 2 steps) was prepared from 2-hydrazinyl-4-((1-phenylcyclohexyl)methoxy)-3-(trifluoromethyl)pyridine (from 6.9.2.) following procedures analogous to steps 6.2.3. and 6.2.4. The crude product was dissolved in a minmum amount of boiling ethyl acetate. The solution was allowed to cool to rt. After 3 h, the crystalline solid was collected by vacuum filtration to afford a white solid. ^{1}H NMR (500 MHz, DMSO-d_6) δ 8.62 (d, *J*=7.8 Hz, 1H), 7.48 (d, *J*=7.5 Hz, 2H), 7.35 (t, *J*=7.8 Hz, 2H), 7.26 - 7.16 (m, 1H), 7.09 (d, *J*=7.8 Hz, 1H), 4.22 (s, 2H), 3.01 (d, *J*=6.9 Hz, 2H), 2.23 (d, *J*=13.9 Hz, 2H), 1.89 - 1.74 (m, 2H), 1.66 - 1.44 (m, 3H), 1.43 - 1.24 (m, 3H), 1.22 - 1.04 (m, 1H), 0.56 - 0.42 (m, 2H), 0.31 - 0.17 (m, 2H); LC–MS $(M+H)^+$ 430.2.

6.10 3-(cyclopropylmethyl)-7-(((1*r*,4*r*)-4-phenylcyclohexyl)oxy)-8-(trifluoromethyl)-[1,2,4]triazolo[4,3-a]pyridine (7i)

6.10.1. 2-chloro-4-((1-phenylcyclohexyl)methoxy)-3-(trifluoromethyl)pyridine. 2-Chloro-4-(((1*r*,4*r*)-4-phenylcyclohexyl)oxy)-3-(trifluoromethyl)pyridine (395 mg, 1.11 mmol, 65 % yield) was prepared from (1*r*,4*r*)-4-phenylcyclohexanol (commercially available) and 2,4-dichloro-3-(trifluoromethyl)pyridine[30] following a procedure analogous to step 6.2.1. ^{1}H NMR (500 MHz, $CDCl_3$) δ 8.33 (d, *J*=5.8 Hz, 1H), 7.37 - 7.30 (m, 2H), 7.26 - 7.19 (m, 3H), 6.93 (d, *J*=6.0 Hz, 1H), 4.55 - 4.42 (m, 1H), 2.64 (tt, *J*=11.9, 3.5 Hz, 1H), 2.35 - 2.23 (m, 2H), 2.13 - 2.02 (m, 2H), 1.83 - 1.70 (m, 2H), 1.70 - 1.59 (m, 2H); LC–MS $(M+H)^+$ 356.1.

6.10.2. 2-hydrazinyl-4-((1*r*,4*r*)-4-phenylcyclohexyloxy)-3-(trifluoromethyl)pyridine. 2-hydrazinyl-4-(((1*r*,4*r*)-4-phenylcyclohexyl)oxy)-3-(trifluoromethyl)pyridine (385 mg, 100 % yield) was prepared from 2-chloro-4-(((1*r*,4*r*)-4-phenylcyclohexyl)oxy)-3-(trifluoromethyl)pyridine (from step 6.10.1.) following a procedure analogous to step 6.2.2. LC–MS $(M+H)^+$ 352.2.

6.10.3. 3-(Cyclopropylmethyl)-7-((1*r*,4*r*)-4-phenylcyclohexyloxy)-8-(trifluoromethyl)-[1,2,4]triazolo[4,3-a]pyridine. The titled compound (147 mg, 64 % yield over 2 steps) was prepared from 2-hydrazinyl-4-(((1*r*,4*r*)-4-phenylcyclohexyl)oxy)-3-(trifluoromethyl)pyridine (from step 6.10.2.) following procedures analogous to steps 6.2.3. and 6.2.4. The product was purified using silica gel column chromatography (100% EtOAc). ^{1}H NMR (500 MHz, $CDCl_3$) δ 8.07 (d, *J*=7.6 Hz, 1H), 7.39 - 7.29 (m, 2H), 7.26 - 7.17 (m, 3H), 6.84 (d, *J*=7.8 Hz, 1H), 4.54 - 4.42 (m, 1H), 3.07 (d, *J*=6.7 Hz, 2H), 2.64 (tt, *J*=12.0, 3.5 Hz, 1H), 2.32 - 2.22 (m, 2H), 2.14 - 2.03 (m, 2H), 1.86 - 1.74 (m, 2H), 1.71 - 1.56 (m, 2H), 1.22 - 1.12 (m, 1H), 0.70 - 0.56 (m, 2H), 0.40 - 0.27 (m, 2H); LC–MS $(M+H)^+$ 416.2.

6.11 3-(cyclopropylmethyl)-7-(3-phenylcyclobutoxy)-8-(trifluoromethyl)-[1,2,4]triazolo[4,3-a]pyridine (7j)

6.11.1. 3-phenylcyclobutanol. Sodium borohydride (108 mg, 2.86 mmol) was added to a stirred solution of 3-phenylcyclobutanone (380 mg, 2.60 mmol) in ethanol (15 mL) maintained in a 0 °C ice bath. After 2 h, the reaction was diluted with water and the pH was adjusted to 2 by the addition of 1 N aqueous hydrochloric acid. The mixture was extracted with ethyl acetate. The combined organics were washed with brine, dried (magnesium sulfate), filtered and concentrated in vacuo to afford 3-phenylcyclobutanol (423 mg, quantitative yield). The product was used without purification. ^{1}H NMR was consistent with the desired product, but suggested a 2:1 (trans/cis) mixture of diastereomers. Data for major diasteromer: ^{1}H NMR (500 MHz, $CDCl_3$) δ 7.33 - 7.31 (m, 2H), 7.25 (d, *J*=7.8 Hz, 3H), 4.35 - 4.28 (m, 1H), 3.03 - 2.95 (m, 1H), 2.84 - 2.77 (m, 2H), 2.07 - 2.01 (m, 2H).

6.11.2. 2-chloro-4-(3-phenylcyclobutoxy)-3-(trifluoromethyl)pyridine. 2-chloro-4-(3-phenylcyclobutoxy)-3-(trifluoromethyl)pyridine (100 mg, 11 % yield) was prepared from 3-phenylcyclobutanol (from step 6.11.1.) and 2,4-dichloro-3-(trifluoromethyl)pyridine[30] following a procedure analogous to step 6.2.1. ^{1}H NMR (500 MHz, $CDCl_3$) δ 8.36 (d, *J*=5.8 Hz, 1H), 7.39 - 7.33 (m, 2H), 7.28 - 7.24 (m, 3H), 6.81 (d, *J*=5.8 Hz, 1H), 4.82 (quin, *J*=7.2 Hz, 1H), 3.31 - 3.22 (m, 1H), 3.06 - 2.97 (m, 2H), 2.41 (tdq, *J*=9.9, 7.5, 2.5 Hz, 2H); LCMS $(M+H)^+$ 328.2.

6.11.3. 2-hydrazinyl-4-(3-phenylcyclobutoxy)-3-(trifluoromethyl)pyridine. 2-hydrazinyl-4-(3-phenylcyclobutoxy)-3-(trifluoromethyl)pyridine (103 mg, quantitative yield) was prepared from 2-chloro-4-(3-phenylcyclobutoxy)-3-(trifluoromethyl)pyridine (from step 6.11.2.) following a procedure analogous to step 6.2.2. LC–MS $(M+H)^+$ 324.2.

6.11.4. 3-(cyclopropylmethyl)-7-(3-phenylcyclobutoxy)-8-(trifluoromethyl)-[1,2,4]triazolo[4,3-a]pyridine. The titled compound (40 mg, 34 % yield over 2 steps) was prepared from 2-hydrazinyl-4-(3-phenylcyclobutoxy)-3-(trifluoromethyl)pyridine (from step 6.11.3.) following procedures analogous to steps 6.2.3. and 6.2.4. The final product was purified by preparative LC-MS. ^{1}H NMR (500 MHz, DMSO-d_6) δ 8.68 (d, *J*=7.6 Hz, 1H), 7.38 - 7.14 (m, 5H), 7.08 (d, *J*=7.6 Hz, 1H), 5.13 (t, *J*=7.0 Hz, 1H), 3.25 - 3.13 (m, 1H), 3.12 - 2.88 (m, 4H), 2.17 (d, *J*=8.9 Hz, 2H), 1.28 - 1.05 (m, 1H), 0.61 - 0.41 (m, 2H), 0.37 - 0.18 (m, 2H); LC–MS $(M+H)^+$ 388.4.

6.12 3-(cyclopropylmethyl)-7-(3-(4-fluorophenyl)cyclobutoxy)-8-(trifluoromethyl)-[1,2,4]triazolo[4,3-a]pyridine (7k)

6.12.1. 3-(4-fluorophenyl)cyclobutanol. Sodium borohydride (0.253 g, 6.70 mmol) was added to a stirred solution of 3-(4-fluorophenyl)cyclobutanone (1.0 g, 6.09 mmol) in ethanol (40 mL) maintained in a 0 °C ice bath. After 2 h, the reaction was diluted with water and the pH was adjusted to 2 by the addition of 1 N aqueous hydrochloric acid. The mixture was extracted with ethyl acetate. The combined organics were washed with brine, dried (magnesium sulfate), filtered and concentrated in vacuo to afford 3-(4-fluorophenyl)cyclobutanol (1.12 g, quantitative yield). The product was used without purification. ^{1}H NMR integration suggested a 6:1 mixture of diastereomers (trans/cis). Data for trans isomer: ^{1}H NMR (500 MHz, $CDCl_3$) δ 7.21 - 7.17 (m, 2H), 7.02 - 6.98 (m, 2H), 4.34 - 4.27 (m, 1H), 3.00 - 2.91 (m, 1H), 2.82 - 2.75 (m, 2H), 2.07 (d, *J*=2.0 Hz, 1H), 2.02 - 1.97 (m, 2H).

6.12.2. 2-chloro-4-(3-(4-fluorophenyl)cyclobutoxy)-3-(trifluoromethyl)pyridine. 2-chloro-4-(3-(4-

fluorophenyl)cyclobutoxy)-3-(trifluoromethyl)pyridine (1.22 g, 59 % yield) was prepared from 3-(4-fluorophenyl)cyclobutanol (from step 6.12.1.) and 2,4-dichloro-3-(trifluoromethyl)pyridine[30] following a procedure analogous to step 6.2.1. ^{1}H NMR (500 MHz, $CDCl_3$) δ 8.35 (d, *J*=5.8 Hz, 1H), 7.24 - 7.19 (m, 2H), 7.07 - 7.01 (m, 2H), 6.79 (d, *J*=5.8 Hz, 1H), 4.80 (t, *J*=7.1 Hz, 1H), 3.28 - 3.19 (m, 1H), 3.04 - 3.00 (m, 2H), 2.39 - 2.32 (m, 2H); LC-MS $(M+H)^+$ = 346.1.

6.12.3. 4-(3-(4-fluorophenyl)cyclobutoxy)-2-hydrazinyl-3-(trifluoromethyl)pyridine. 4-(3-(4-fluorophenyl)cyclobutoxy)-2-hydrazinyl-3-(trifluoromethyl)pyridine (486 mg, quantitative yield) was prepared from 2-chloro-4-(3-(4-fluorophenyl)cyclobutoxy)-3-(trifluoromethyl)pyridine (from step 6.12.2.) following a procedure analogous to step 6.2.2. LC–MS $(M+H)^+$ 345.1.

6.12.4. 3-(cyclopropylmethyl)-7-(3-(4-fluorophenyl)cyclobutoxy)-8-(trifluoromethyl)-[1,2,4]triazolo[4,3-a]pyridine. The titled compound (103 mg, 38 % yield over 2 steps) was prepared from 4-(3-(4-fluorophenyl)cyclobutoxy)-2-hydrazinyl-3-(trifluoromethyl)pyridine (from step 6.12.3.) following procedures analogous to steps 6.2.3. and 6.2.4. The final product was purified using silica gel column chromatography (100% EtOAc). ^{1}H NMR (500 MHz, $CDCl_3$) δ 8.09 (d, *J*=7.6 Hz, 1H), 7.26 - 7.20 (m, 2H), 7.08 - 7.00 (m, 2H), 6.72 (d, *J*=7.8 Hz, 1H), 4.87 (quin, *J*=7.2 Hz, 1H), 3.27 - 3.17 (m, 1H), 3.09 (d, *J*=6.7 Hz, 2H), 3.04 - 2.94 (m, 2H), 2.48 - 2.37 (m, 2H), 1.23 - 1.12 (m, 1H), 0.68 - 0.61 (m, 2H), 0.37 - 0.32 (m, 2H); LC–MS $(M+H)^+$ 406.3.

6.13 (±)-3-(Cyclopropylmethyl)-7-(((1S,2S)-2-(4-fluorophenyl)cyclopropyl)methoxy)-8-(trifluoromethyl)-[1,2,4]triazolo[4,3-a]pyridine (13l)

6.13.1. methyl *trans*-2-(4-fluorophenyl)cyclopropanecarboxylate. A mixture of *trans*-2-(4-fluorophenyl)cyclopropanecarboxylic acid (commercially available, 159 mg, 0.88 mmol), methanol (5.0 ml), and sulfuric acid (0.15 ml, 2.81 mmol) was heated in a sealed vial at 72 °C for 18 h. The reaction was carefully neutralized by the addition of aqueous 10 % sodium carbonate solution. The resulting mixture was evaporated in vacuo. The residue was partitioned between ethyl acetate and water. The aqueous phase was extracted with ethyl acetate. The combined organic layers were washed with brine, dried (sodium sulfate), filtered, and concentrated in vacuo to afford methyl *trans*-methyl 2-(4-fluorophenyl)cyclopropanecarboxylate (167 mg, 97 % yield) as a light brown oil. ^{1}H NMR (500 MHz, $CDCl_3$) δ 7.11 - 7.06 (m, 2H), 7.01 - 6.95 (m, 2H), 3.74 (s, 3H), 2.53 (ddd, *J*=9.3, 6.4, 4.1 Hz, 1H), 1.87 (ddd, *J*=8.4, 5.2, 4.2 Hz, 1H), 1.64 - 1.58 (m, 1H), 1.32 - 1.25 (m, 2H).

6.13.2. (*trans*-2-(4-fluorophenyl)cyclopropyl)methanol. (*trans*-2-(4-fluorophenyl)cyclopropyl)methanol (119 mg, 83 % yield) was prepared from *trans*-methyl 2-(4-fluorophenyl)cyclopropanecarboxylate (from step 6.13.1.) following a procedure analogous to step 6.3.1. ^{1}H NMR (500 MHz, $CDCl_3$) δ 7.10 - 7.01 (m, 2H), 6.98 - 6.93 (m, 2H), 3.63 (d, *J*=6.7 Hz, 2H), 1.86 - 1.80 (m, 1H), 1.68 (br. s., 1H), 1.45 - 1.37 (m, 1H), 0.97 - 0.85 (m, 3H).

6.13.3. (±)-2-chloro-4-(((1S,2S)-2-(4-fluorophenyl)cyclopropyl)methoxy)-3-(trifluoromethyl)pyridine. (±)-2-chloro-4-(((1S,2S)-2-(4-fluorophenyl)cyclopropyl)methoxy)-3-(trifluoromethyl)pyridine (183 mg, 76 % yield) was prepared from (*trans*-2-(4-fluorophenyl)cyclopropyl)methanol (from step 6.13.2.) and 2,4-dichloro-3-(trifluoromethyl)pyridine[32] following a procedure analogous to step 6.2.1. (a). ^{1}H NMR (500 MHz, $CDCl_3$) δ 8.34 (d, *J*=5.8 Hz, 1H), 7.12 - 7.07 (m, 2H), 7.01 - 6.94 (m, 2H), 6.88 (d, *J*=5.8 Hz, 1H), 4.26 (dd, *J*=9.9, 6.0 Hz, 1H), 4.07 (dd, *J*=9.8, 6.9 Hz, 1H), 1.57 - 1.49 (m, 1H), 1.16 - 1.06 (m, 2H), 0.96 - 0.83 (m, 1H).

6.13.4. (±)-4-(((1*S*,2*S*)-2-(4-fluorophenyl)cyclopropyl)methoxy)-2-hydrazinyl-3-(trifluoromethyl)pyridine. (±)-4-(((1S,2*S*)-2-(4-fluorophenyl)cyclopropyl)methoxy)-2-hydrazinyl-3-(trifluoromethyl)pyridine (181 mg, quantitative yield) was prepared from (±)-2-chloro-4-(((1S,2S)-2-(4-fluorophenyl)cyclopropyl)methoxy)-3-(trifluoromethyl)pyridine (from step 6.13.3.) following a procedure analogous to step 6.2.2. ^{1}H NMR (500 MHz, METHANOL-d_4) δ 8.19 - 8.16 (m, 1H), 7.17 - 7.13 (m, 2H), 6.98 (s, 2H), 6.59 - 6.53 (m, 1H), 4.29 - 4.23 (m, 1H), 4.10 - 4.03 (m, 1H), 1.55 - 1.46 (m, 1H), 1.11 - 1.04 (m, 2H), ^{19}F NMR m -56.19, -119.87; LC–MS $(M+H)^+$ 342.1.

6.13.5. (±)-3-(Cyclopropylmethyl)-7-(((1S,2S)-2-(4-fluorophenyl)cyclopropyl)methoxy)-8-(trifluoromethyl)-[1,2,4]triazolo[4,3-a]pyridine. The titled compound (80 mg, 20 % yield over 2 steps) was prepared from (±)-4-(((1S,2S)-2-(4-fluorophenyl)cyclopropyl)methoxy)-2-hydrazinyl-3-(trifluoromethyl)pyridine (from step 6.13.4.) following procedures analogous to steps 6.2.3. and 6.2.4. The final product was purified by silica-gel column chromatography (0-100% ethyl acetate) and reverse phase preparatory HPLC. ^{1}H NMR (500 MHz, METHANOL-d_4) δ 8.56 (d, *J*=7.8 Hz, 1H), 7.21 (d, *J*=7.5 Hz, 1H), 7.17 - 7.11 (m, 2H), 7.01 - 6.93 (m, 2H), 4.47 (dd, *J*=10.3, 6.3 Hz, 1H), 4.29 (dd, *J*=10.2, 7.3 Hz, 1H), 3.07 (d, *J*=6.9 Hz, 2H), 2.10 - 2.04 (m, 1H), 1.62 - 1.50 (m, 1H), 1.30 - 1.18 (m, 1H), 1.16 - 1.07 (m, 2H), 0.66 - 0.59 (m, 2H), 0.39 - 0.32 (m, 2H); LC–MS $(M+H)^+$ 406.1.

6.14 (±)-3-(Cyclopropylmethyl)-7-(((1S,2S)-2-(4-chlorophenyl)cyclopropyl)methoxy)-8-(trifluoromethyl)-[1,2,4]triazolo[4,3-a]pyridine (7m)

6.14.1. methyl *trans*-2-(4-chlorophenyl)cyclopropanecarboxylate. A mixture of *trans*-2-(4-chlorophenyl)cyclopropanecarboxylic acid (commercially available, 1.0 g, 5.09 mmol), methanol (29.1 ml), and sulfuric acid (0.813 ml, 15.3 mmol) was heated in a sealed vial at 72 °C for 18 h. The reaction was carefully neutralized by the addition of aqueous 10 % sodium carbonate solution. The resulting mixture was evaporated in vacuo. The residue was partitioned between ethyl acetate and water. The aqueous phase was extracted with ethyl acetate. The combined organic layers were washed with brine, dried (sodium sulfate), filtered, and concentrated in vacuo to afford methyl *trans*-2-(4-chlorophenyl)cyclopropanecarboxylate (1.07 g, quantitative yield) as a light brown oil. ^{1}H NMR (500 MHz, $CDCl_3$) δ 7.29 - 7.26 (m, 2H), 7.07 - 7.03 (m, 2H), 3.74 (s, 3H), 2.52 (ddd, *J*=9.3, 6.4, 4.2 Hz, 1H), 1.89 (ddd, *J*=8.5, 5.3, 4.3 Hz, 1H), 1.65 - 1.60 (m, 1H), 1.33 - 1.29 (m, 1H).

6.14.2. (*trans*-2-(4-chlorophenyl)cyclopropyl)methanol. (*trans*-2-(4-chlorophenyl)cyclopropyl)methanol (582 mg, 3.19 mmol, 62.8 % yield) was prepared from *trans*-methyl 2-(4-fluorophenyl)cyclopropanecarboxylate (from step 6.14.1.) following a procedure analogous to step 6.3.1. LC–MS $(M-H_2O+H)^+$ 165.0.

6.14.3. (±)-2-Chloro-4-(((1*S*,2*S*)-2-(4-chlorophenyl)cyclopropyl)methoxy)-3-(trifluoromethyl)pyridine. (±)-2-Chloro-4-(((1*S*,2*S*)-2-(4-chlorophenyl)cyclopropyl)methoxy)-3-(trifluoromethyl)pyridine

(450 mg, 76 % yield) was prepared from (*trans*-2-(4-chlorophenyl)cyclopropyl)methanol (from step 6.14.2.) and 2,4-dichloro-3-(trifluoromethyl)pyridine[32] following a procedure analogous to step 6.2.1. ^{1}H NMR (500 MHz, $CDCl_3$) δ 8.38 (d, *J*=4.7 Hz, 1H), 7.28 - 7.25 (m, 2H), 7.09 - 7.05 (m, 2H), 6.89 (d, *J*=4.6 Hz, 1H), 4.27 (dd, *J*=9.8, 6.1 Hz, 1H), 4.16 - 4.07 (m, 1H), 2.07 - 2.01 (m, 1H), 1.56 (dd, *J*=12.6, 6.3 Hz, 1H), 1.18 - 1.10 (m, 2H).

6.14.4. (±)-4-((1-(4-chlorophenyl)cyclopropyl)methoxy)-2-hydrazinyl-3-(trifluoromethyl)pyridine. **(±)**-4-((1-(4-chlorophenyl)cyclopropyl)methoxy)-2-hydrazinyl-3-(trifluoromethyl)pyridine (451 mg, quantitative yield) was prepared from (±)-2-chloro-4-(((1*S*,2*S*)-2-(4-chlorophenyl)cyclopropyl)methoxy)-3-(trifluoromethyl)pyridine (from step 6.14.3.) following a procedure analogous to step 6.2.2. LC–MS $(M+H)^+$ 358.0.

6.14.5. (±)-7-(((1*S*,2*S*)-2-(4-chlorophenyl)cyclopropyl)methoxy)-3-(cyclopropylmethyl)-8-(trifluoromethyl)-[1,2,4]triazolo[4,3-a]pyridine. The titled compound (145 mg, 26 % yield over 2 steps) was prepared from **(±)**-4-((1-(4-chlorophenyl)cyclopropyl)methoxy)-2-hydrazinyl-3-(trifluoromethyl)pyridine (from step 6.14.4.) following procedures analogous to steps 6.2.3. and 6.2.4. The final product was purified by silica-gel column chromatography (0-100% ethyl acetate/hexanes). ^{1}H NMR (500 MHz, DMSO-d_6) δ 8.70 (d, *J*=7.8 Hz, 1H), 7.33 - 7.27 (m, 2H), 7.21 (d, *J*=7.8 Hz, 1H), 7.16 - 7.11 (m, 2H), 4.46 - 4.40 (m, 1H), 4.33 (dd, *J*=10.6, 7.2 Hz, 1H), 3.04 (d, *J*=6.9 Hz, 2H), 2.08 - 2.01 (m, 1H), 1.60 - 1.51 (m, 1H), 1.22 - 1.14 (m, 1H), 1.13 - 1.07 (m, 2H), 0.54 - 0.48 (m, 2H), 0.30 - 0.25 (m, 2H); LC–MS $(M+H)^+$ 421.8.

6.15 (+)-3-(cyclopropylmethyl)-7-(((1S,2S)-2-(4-chlorophenyl)cyclopropyl)methoxy)-8-(trifluoromethyl)-[1,2,4]triazolo[4,3-a]pyridine ((+)-7m) and (-)-3-(cyclopropylmethyl)-7-(((1R,2R)-2-(4-chlorophenyl)cyclopropyl)methoxy)-8-(trifluoromethyl)-[1,2,4]triazolo[4,3-a]pyridine ((-)-7m)

6.15.1. (+)-3-(cyclopropylmethyl)-7-(((1S,2S)-2-(4-chlorophenyl)cyclopropyl)methoxy)-8-(trifluoromethyl)-[1,2,4]triazolo[4,3-a]pyridine ((+)-7m) and (-)-3-(cyclopropylmethyl)-7-(((1R,2R)-2-(4-chlorophenyl)cyclopropyl)methoxy)-8-(trifluoromethyl)-[1,2,4]triazolo[4,3-a]pyridine ((-)-7m). A sample of (±)-7-(((1S,2S)-2-(4-chlorophenyl)cyclopropyl)methoxy)-3-(cyclopropylmethyl)-8-(trifluoromethyl)-[1,2,4]triazolo[4,3-a]pyridine (from step 6.14.5., 233 mg) was purified using chiral preparatory HPLC to afford 61 mg of (-)-13m (first eanantiomer to elute) and 60 mg of (+)-13m (second enantiomer to elute). HPLC Method: ChiralCel OD (21 x 250 mm, 10 uM), 10 % ethanol / 90 % heptane (with 0.1 % diethylamine), 15 mL/min, absorbance 254 nm. The absolute stereochemistry of (+)-13m was confirmed as (1*S*,2*S*) through an independent asymmetric synthesis (step 6.16). The stereochemistry of (-)-13m was assigned as (1*R*,2*R*) by default. **(+)-7m**: ^{1}H NMR (500 MHz, DMSO-d_6) δ 8.69 (d, *J*=7.6 Hz, 1H), 7.35 - 7.25 (m, *J*=8.5 Hz, 2H), 7.20 (d, *J*=7.6 Hz, 1H), 7.17 - 7.07 (m, *J*=8.5 Hz, 2H), 4.42 (dd, *J*=10.7, 6.7 Hz, 1H), 4.32 (dd, *J*=10.7, 7.3 Hz, 1H), 3.03 (d, *J*=7.0 Hz, 2H), 2.11 - 1.97 (m, 1H), 1.60 - 1.47 (m, 1H), 1.27 - 1.13 (m, 1H), 1.09 (t, *J*=7.0 Hz, 2H), 0.58 - 0.44 (m, 2H), 0.27 (q, *J*=4.7 Hz, 2H); LC–MS $(M+H)^+$ 421.8. **(-)-7m**: ^{1}H NMR (500 MHz, DMSO-d_6) δ 8.69 (d, *J*=7.6 Hz, 1H), 7.35 - 7.25 (m, *J*=8.5 Hz, 2H), 7.20 (d, *J*=7.6 Hz, 1H), 7.17 - 7.07 (m, *J*=8.5 Hz, 2H), 4.42 (dd, *J*=10.7, 6.7 Hz, 1H), 4.32 (dd, *J*=10.7, 7.3 Hz, 1H), 3.03 (d, *J*=7.0 Hz, 2H), 2.11 - 1.97 (m, 1H), 1.60 - 1.47 (m, 1H), 1.27 - 1.13 (m, 1H), 1.09 (t, *J*=7.0 Hz, 2H), 0.58 - 0.44 (m, 2H), 0.27 (q, *J*=4.7 Hz, 2H); LC–MS $(M+H)^+$ 421.8.

6.16 (+)-3-(cyclopropylmethyl)-7-(((1S,2S)-2-(4-chlorophenyl)cyclopropyl)methoxy)-8-(trifluoromethyl)-[1,2,4]triazolo[4,3-a]pyridine (+)-(7m)

6.16.1. (E)-3-(4-chlorophenyl)acryloyl chloride. Thionyl chloride (8.79 mL, 120 mmol) was added to a 100 mL round-bottomed flask charged with a suspension of (E)-3-(4-chlorophenyl)acrylic acid **(14)** (10 g, 54.8 mmol) in anhydrous dichloromethane (200 mL) under nitrogen. The reaction mixture was stirred at rt for 12h. The reaction mixture was concentrated *in vacuo* to afford the crude product (E)-3-(4-chlorophenyl)acryloyl chloride (11.05 g, quantitative yield) as a white solid. ^{1}H NMR (500MHz, $CDCl_3$) δ 7.81 (d, *J*=15.6 Hz, 1H), 7.57 - 7.51 (m, 2H), 7.47 - 7.41 (m, 2H), 6.65 (d, *J*=15.6 Hz, 1H).

6.16.2. (E)-3-(4-chlorophenyl)-1-((3aR,6R,7aS)-8,8-dimethyl-2,2-dioxidohexahydro-1H-3a,6-methanobenzo[c]isothiazol-1-yl)prop-2-en-1-one (15). To a cold (0°C) solution of the (E)-3-(4-chlorophenyl)acryloyl chloride (from step 5.16.1., 11 g, 54.7 mmol) in dichloromethane (25 mL), was added a solution of (3aR,6R,7aS)-8,8-dimethylhexahydro-1H-3a,6-methanobenzo[c]isothiazole 2,2-dioxide (12.96 g, 60.2 mmol) and Et_3N (22.88 mL, 164 mmol) in dichloromethane (100 mL) dropwise. After the addition was complete, the ice bath was removed, and stirring was continuted for 2 h. The reaction was diluted with dichloromethane, then washed well with water, saturated sodium bicarbonate, brine, dried over sodium sulfate, and concentrated to give a beige solid. The solid was recrystallized from hot EtOH to give (E)-3-(4-chlorophenyl)-1-((3aR,6R,7aS)-8,8-dimethyl-2,2-dioxidohexahydro-1H-3a,6-methanobenzo[c]isothiazol-1-yl)prop-2-en-1-one (17.03 g, 82 % yield) as a white crystalline solid. ^{1}H NMR (500MHz, $CDCl_3$) δ 7.75 (d, *J*=15.4 Hz, 1H), 7.56 - 7.50 (m, 2H), 7.40 - 7.34 (m, 2H), 7.16 (d, *J*=15.4 Hz, 1H), 4.01 (dd, *J*=7.6, 5.0 Hz, 1H), 3.60 - 3.46 (m, 2H), 2.26 - 2.13 (m, 2H), 2.02 - 1.90 (m, 3H), 1.52 - 1.38 (m, 2H), 1.23 (s, 3H), 1.02 (s, 3H); LC–MS $(M+H)^+$ 380.2.

6.16.3. ((1S,2S)-2-(4-chlorophenyl)cyclopropyl)((6R,7aR)-8,8-dimethyl-2,2-dioxidohexahydro-1H-3a,6-methanobenzo[c]isothiazol-1-yl)methanone (16). N-methyl-N'-nitro-N-nitrosoguanidine (23.24 g, 158 mmol) was carefully added portionwise over 20 min to a swirled bilayer of diethyl ether (500 mL) and 5 N NaOH (500 ml) in a plastic coated 2000 mL Erlenmyer flask that was placed in an ice-water bath behind a blast shield. After 15 min, when all bubbling had ceased the ether layer was decanted into a separate 2000 mL Erlenmyer flask charged with ~80 g of KOH pellets in an ice-water bath. The yellow solution was swirled occasionally for 10 min, then the ethereal diazomethane solution was transferred to a diazo-addition funnel suspended above a new 2000 mL Erlenmyer fask charged with a gently stirred solution of (E)-3-(4-chlorophenyl)-1-((3aR,6R,7aS)-8,8-dimethyl-2,2-dioxidohexahydro-1H-3a,6-methanobenzo[c]isothiazol-1-yl)prop-2-en-1-one (from step 6.16.2., 10 g, 26.3 mmol) and palladium(II) acetate (0.177 g, 0.790 mmol) in DCM (66 mL) maintained at -10 °C. After complete addition, the mixture was allowed to warm to rt and for 16h. The reaction was chilled to 0 °C and quenched with acetic acid. The reaction was filtered over celite, poured into a solution of saturated sodium bicarbonate, and extracted with ethyl acetate (3 x 250 mL). The combined organic layers were washed with brine, dried over magnesium sulfate, and concentrated *in vacuo*. The crude product was purified by silica gel column chromatography (0-15% ethyl acetate/hexanes) and recrystallization from ethyl acetate/hexanes to afford ((1S,2S)-2-

(4-chlorophenyl)cyclopropyl)((6R,7aR)-8,8-dimethyl-2,2-dioxidohexahydro-1H-3a,6-methanobenzo[c]isothiazol-1-yl)methanone (7.6 g, 73% yield) as a white crystalline solid. ^{1}H NMR (500MHz, $CDCl_3$) δ 7.28 - 7.25 (m, 2H), 7.18 - 7.15 (m, 2H), 3.93 (dd, *J*=7.8, 4.9 Hz, 1H), 3.53 (d, *J*=13.7 Hz, 1H), 3.46 (d, *J*=13.9 Hz, 1H), 2.61 - 2.51 (m, 2H), 2.18 - 2.12 (m, 1H), 2.11 - 2.05 (m, 1H), 1.97 - 1.88 (m, 3H), 1.83 - 1.77 (m, 1H), 1.47 - 1.32 (m, 3H), 1.22 (s, 3H), 1.00 (s, 3H); LC–MS $(M+H)^+$ 394.2.

6.16.4. ((1S,2S)-2-(4-chlorophenyl)cyclopropyl)methanol (17). To a stirring suspension of LAH (0.915 g, 24.12 mmol) in THF (100 mL) was added dropwise a solution of ((1S,2S)-2-(4-chlorophenyl)cyclopropyl)((6R,7aR)-8,8-dimethyl-2,2-dioxidohexahydro-1H-3a,6-methanobenzo[c]isothiazol-1-yl)methanone (from step 5.16.3., 7.6 g, 19.29 mmol) in THF (20 mL) and the resulting mixture was stirred at -40 °C under nitrogen. After complete addition, the reaction mixture was stirred for 1h. The reaction was quenched by the addition of aqueous ammonium hydroxide solution. The reaction mixture was slurried in a mixture of water and ethyl acetate and filtered. The layers were then separated, the aqueous layer was washed again with ethyl acetate, and the combined organic layers were washed with brine and dried over magnesium sulfate. The drying agent was filtered off and the solvent was concentrated in vacuo to afford ((1S,2S)-2-(4-chlorophenyl)cyclopropyl)methanol (3.5 g, 99 % yield). LC–MS $(M-H20+H)^+$ 165.2.

6.16.5. 2-chloro-4-(((1S,2S)-2-(4-chlorophenyl)cyclopropyl)methoxy)-3-(trifluoromethyl)pyridine. 2-chloro-4-(((1S,2S)-2-(4-chlorophenyl)cyclopropyl)methoxy)-3-(trifluoromethyl)pyridine (3.25 g, 66 % yield) was prepared from (((1S,2S)-2-(4-chlorophenyl)cyclopropyl)methanol (from step 6.16.4.) and 2,4-dichloro-3-(trifluoromethyl)pyridine[32] following a procedure analogous to step 6.2.1. ^{1}H NMR (500MHz, $CDCl_3$) δ 8.37 (d, *J*=5.8 Hz, 1H), 7.28 - 7.25 (m, 2H), 7.09 - 7.06 (m, 2H), 6.88 (d, *J*=5.8 Hz, 1H), 4.26 (dd, *J*=9.9, 6.1 Hz, 1H), 4.09 (dd, *J*=9.8, 6.8 Hz, 1H), 2.07 - 2.01 (m, 1H), 1.59 - 1.54 (m, 1H), 1.16 - 1.11 (m, 2H).

6.16.6. 4-(((1S,2S)-2-(4-chlorophenyl)cyclopropyl)methoxy)-2-hydrazinyl-3-(trifluoromethyl)pyridine. 4-(((1S,2S)-2-(4-chlorophenyl)cyclopropyl)methoxy)-2-hydrazinyl-3-(trifluoromethyl)pyridine (2.91 g, 91 % yield) was prepared from 2-chloro-4-(((1S,2S)-2-(4-chlorophenyl)cyclopropyl)methoxy)-3-(trifluoromethyl)pyridine (from step 6.16.5.) following a procedure analogous to step 6.2.2. LC–MS $(M+H)^+$ 358.2.

6.16.7. (+)-7-(((1S,2S)-2-(4-chlorophenyl)cyclopropyl)methoxy)-3-(cyclopropylmethyl)-8-(trifluoromethyl)-[1,2,4]triazolo[4,3-a]pyridine ((+)-7m). The titled compound (1.77 g, 50 % yield over 2 steps) was prepared from 4-(((1S,2S)-2-(4-chlorophenyl)cyclopropyl)methoxy)-2-hydrazinyl-3-(trifluoromethyl)pyridine (from step 6.16.6.) following procedures analogous to steps 6.2.3. and 6.2.4. The final product was purified by silica-gel column chromatography (0-100% ethyl acetate/hexanes) and recrystallized with hot EtOH. ^{1}H NMR (500MHz, $CDCl_3$) δ 8.10 (d, *J*=7.6 Hz, 1H), 7.27 - 7.24 (m, 2H), 7.09 - 7.03 (m, 2H), 6.81 (d, *J*=7.6 Hz, 1H), 4.33 (dd, *J*=9.9, 6.1 Hz, 1H), 4.20 (dd, *J*=9.9, 6.7 Hz, 1H), 3.08 (d, *J*=6.7 Hz, 2H), 2.08 - 2.00 (m, 1H), 1.60 - 1.51 (m, 1H), 1.20 - 1.12 (m, 3H), 0.67 - 0.62 (m, 2H), 0.36 - 0.32 (m, 2H); LC–MS $(M+H)^+$ 421.8.

7.0 In Vitro Biology Materials and Methods

7.1 $mGlu_2$ PAM competition radioligand binding assay

HEK293 cells stably-expressing the human $mGlu_2$ receptor and rat glutamate transporter (GLAST) were used as the cell membrane source. Cell pellets were homogenized at 4 °C in hypotonic lysis buffer (50 mM TRIS pH 7.4, 10 mM $MgCl_2$, 2 mM EGTA and 0.1% (v/v) Sigma Protease Inhibitor Cocktail) followed by centrifugation at 32,000 x g for 30 min. The supernatant was discarded and the pellet was washed once in lysis buffer and centrifuged at 32,000 x g for 30 min. This pellet was then resuspended in lysis buffer and protein concentrations were determined using bovine serum albumin as a standard. The membranes were aliquoted and frozen in dry ice/ethanol and kept at -80°C until the day of the assay.

Frozen aliquots of membrane homogenate were thawed, homogenized and resuspended at 0.2 mg/ml protein in assay buffer (20 mM TRIS-Cl pH 7.4, 5 mM KCl, 2 mM $CaCl_2$, 2 mM $MgCl_2$, and 0.005% Triton X-100) at 4 °C. Competition binding experiments were performed using 7.5 nM [^{3}H]-JNJ-40068782 (Specific activity 28.1 Ci/mmol) in the presence 10 concentrations (in duplicate) of test compound. Addition of 1 uM $mGlu_{2/3}$ orthosteric agonist LY379268 was used to increase assay window without altering test compound IC_{50}s and was included in the buffer. Test compound, membranes (20 ug/well) and radioligand were sequentially added to the wells of a 96 well plate and incubated for 30 minutes at room temperature. Non-specific binding was defined with 10 µM MPPTS. The assay was terminated by the addition of 5 mL of ice-cold wash buffer (50 mM TRIS-Cl pH 7.4 and 0.1% BSA) and rapid filtration through a Brandel Cell Harvester using Whatman GF/B filters presoaked in 0.3% PEI. After 3 rapid washes, the filter was punched onto a 96 well microbeta sample plate, 200 µl/well of Packard Ultima GoldXR scintillation fluid added and the filters soaked overnight. The filter pads were then counted in a LKB Trilux liquid scintillation counter.

IC_{50} values were determined using non-linear regression in Curvemaster. Ki (apparent) values were calculated using the method of Cheng and Prusoff.

The Kd value of the radiolabel +/- LY379268 was 7.78 nM ± 2.09 and 5.56 nM ± 1.36, respectively.

The constitutive activity for LY341495 in this assay was IC_{50} = 1.48 nM.

7.2 $mGlu_2$ and $mGlu_3$ cAMP functional assays

Functional assays with human $mGlu_2$ were carried out using the same HEK293 cell line that was used for $mGlu_2$ PAM binding. The cell line provided a robust and sensitive assay platform, but also possessed significant $mGlu_2$ receptor constituitive activity in the cAMP assay. Modifications to the assay to eliminate constituitive activity (see below) preserved the ability to evaluate functional allosteric activity, but did not allow unambiguous determination of the nature of the activity (PAM vs allosteric agonist). Therefore these studies were carried out in the FLIPR assay (described later in the methods). The day before a study, cells were grown in MEM without glutamine (GIBCO MEM12360) with 10% FBS (dialyzed) and 1% pennicillin/streptomycin. On the day of the experiment the media was removed, the cells were washed in PBS and they were trypsinized to remove them from the plate. After adding media to stop the trypsin the cells were centrifuged at 800 x g for 10 minutes and the cell pellet was resuspended in stimulation buffer (Hanks Balanced Salt Solution pH 7.0, 20 mM HEPEs, 2.0 mM $CaCl_2$, 5 mM $MgCl_2$, 1 mM IMBX, 1 µM forskolin and 1µM LY341495) at 1.25 x10^6 cells/per ml. Addition of orthosteric

antagonist LY341495 to the stimulation buffer reduced $mGlu_2$ cell line constituitive activity and improved assay window and consistency, while not altering test compound potency. Compounds were added to white non-binding surface 384 well plates (Corning 3574) as 10 concentration dose responses (in duplicate). Cells in stimulation buffer were then dispensed into the plate and allowed to incubate at RT for 30 minutes. Cells were lysed with addition of Lysis buffer (50mM Phosphate Buffer pH 7.0, 800mM Potassium Fluoride, 0.2% BSA, and 1.0% Triton) containing D2 and cryptate antibodies diluted 1:40 from the CYSBIO dynamic cAMP kit. Cells lysates further incubated for 1 h at RT and were then evaluated using a Perkin Elmer Viewlux. The mGluR3 functional assays were carried out in the same manner except using an HEK293 cell pool expressing human mGluR3 and the glutamate transporter GLAST. Imaging data from both assays was converted to cAMP levels using a cAMP standard curve and IC_{50} values were determined using non-linear regression in Curvemaster.

7.3 $mGlu_2$ FLIPR glutamate shift functional assays

Glutamate shift functional assays were carried out using HEK293 cells stably expressing a humanized form of monkey $mGlu_2$ and a chimeric Gqi_5 G protein which converts Gi signalling to the Gq pathway. The humanized monkey $mGlu_2$ was identical to human $mGlu_2$ with the exception of a conservative amino acid change at the C terminus (Leu846Val). Humanized monkey $mGlu_2$ cells were plated the day before the assay at 40,000 cells per well in 384 well clear bottom plates in glutamine free Gibco MEM media (12360) with 10% dialyzed FBS and 1% pennicillin/streptomycin. The day of the assay the media was removed and replaced with assay buffer (Hanks Balanced Salt Solution, 20 mM HEPES, 2 mM $CaCl_2$, 1 mM $MgCl_2$, 2.5 mM Probenecid, and 5 μM Fluo-4) and incubated at 37 °C for 60 min. The standard assay format was 4 glutamate dose response curves for each test compound (made up of a vehicle dose response and dose responses with three test compound concentrations). Test compound concentrations were adjusted as needed to capture maximal PAM activity. Test compounds were prepared in DMSO and added directly to the assay plates using an ECHO acoustic dispenser and allowed to incubate for 10 minutes at RT. A FLIPR plate reader system was used to dispense the glutamate concentration curves (prepared in assay buffer without Probenecid and Fluo-4) and fluorescence was measured for 3 minutes. Peak fluorescence was normalized against a 100 μM glutamate positive control and concentration response curves were generated using non-linear regression in Loadmaster. Fold shift values were determined by dividing the EC_{50} of glutamate with vehicle treatment by the EC_{50} of the most left shifted glutamate curve in the presence of compound. Curves with a low Y-max (less than 70%, suggesting assay desensitization) were not used in the calculation.

7.4 $mGlu_2$ FLIPR agonist assay

Assays were carried out in a similar manner to the Glutamate shift assays (see above). In the agonist assay compound serial dilutions were added to the plate using the FLIPR and immediately scanned for 3 minutes. The peak fluorescence at each dilution was normalized to 100 uM glutamate (maximal response). In the PAM assay the compound serial dilutions were added to the cells in the plate using the ECHO acoustic dispenser. After a 10 minute preincubation an EC10-20 of glutamate was added to the plate using the FLIPR and the plate was scanned as described previously. IC_{50} values in both assays were determined using non-linear regression in Curvemaster.

8.0 In Vivo Biology Materials and Methods

8.1 Subjects

Unless otherwise specified, animal studies were conducted in group housed (n=3-4), C57Bl/6J male mice (20-30g; Jackson Laboratories, Bar Harbor, ME) held in colony rooms maintained at constant temperature (21 ± 2 °C), and humidity (50 ± 10%) and illuminated for 12 h per day (lights on at 0600 hours). Animals had ad libitum access to food and water throughout the studies. Behavioral studies were conducted between 0700 and 1500 hours. Animals were maintained in accordance with the guidelines of the Animal Care and Use Committee of the Bristol-Myers Squibb Company, and the "Guide for the Care and Use of Laboratory Animals" published by the National Institutes of Health. Research protocols were approved by the Bristol-Myers Squibb Company Animal Care and Use Committee.

8.2 Spontaneous and PCP-Stimulated Locomotion

Mice were habituated to Tru Scan locomotor arenas (Coulbourn Instruments, Allentown, PA) for 90 minutes under low light conditions (30 lux). Following habituation, all mice were treated with vehicle, BMT-133218 (1 to 10 mg/kg, p.o.), or the assay positive control risperidone (0.056 mg/kg, s.c.) and returned to the activity monitors for 30 minutes. Mice were then dosed with saline or PCP (3.2 mg/kg, s.c., in saline, Sigma-Aldrich, St. Louis, MO) and returned to the activity monitors for 2 h. Brain and plasma samples were collected from satellite animals at a time point corresponding to the peak PCP response (1 hr post-PCP), stored at -80 C, and analyzed for compound brain and plasma concentrations. BMT-133218 was prepared in 10% DMSO/18% TPGS/72% water, and risperidone was prepared in 0.3% tartaric acid. Distance travelled (cm) data was collected in five minute bins and summed across the 2-hr PCP phase. Data were analyzed using one-way Analysis of Variance (ANOVA) followed by post-hoc Dunnett's tests.

8.3 Two Trial Y maze

For these experiments, male C57Bl6/Tac mice (20-27g) were used. Experimental methods were adapted from those reported in the literature.[33] Testing was conducted in a grey polyethylene plastic Y maze that had 3 arms, 2 of 40 cm length (test arms) and 1 of 20 cm length (start arm). Each arm had distinct visual cues covering the walls and a removable partition to occlude the arm as needed. The test consisted of two trials: a forced choice trial followed by a free-choice trial. For the forced choice trial only the start arm and one test arm was open with access to the 2nd test arm blocked by the partition. Individual subjects were placed in the start arm and allowed to explore the open test arm for 8 min after which they were removed from the maze, placed in a holding cage and the maze was cleaned. Animals were then immediately placed back on the Y maze for the free choice trial and allowed to explore all open arms for 4 min. The protocol was thus designed for minimal delay between the forced choice and free choice trials. Animal behavior was video recorded during both trials and the time spent in the previously accessible arm (ie familiar arm) and the previously blocked arm (ie novel arm) determined during the free choice trial using Cleversys software.

Results for the free choice trial are presented as the mean ± SEM percentage of time spent exploring the novel arm. The percent time was calculated for each individual subject using the formula: % novel time = novel time/(novel + familiar time) x 100 and was analyzed by one-way ANOVA followed by Dunnett's post-hoc test. The mean time spent exploring the novel or familiar arm was analyzed for each treatment group using a within subjects t-test. Data analysis was conducted using

Graphpad Prism (v5.0, San Diego, CA) with significance set at $p<0.05$.

BMT-133218 was dissolved in 10% DMSO/ 18% TPGS/ 72% water on the day of testing. Vehicle or $mGlu_2$ PAM treatment was administered orally 30 minutes prior to MK-801 (0.05 mg/kg, s.c.) and 60 minutes prior to the forced choice trial. Doses of BMT-133218 tested were 1, 3, and 10 mg/kg (p.o.). For the positive control, mice were pre-treated with the α7 nACh receptor full agonist, PNU-282987 (10 mg/kg, s.c.) 5 minutes prior to the MK-801 injection. A satellite group of animals was sacrificed and plasma samples collected and stored at -80 ºC prior to measurement of drug concentrations.

8.4 Reversal of MK-801-Induced Deficits in Set Shift Performance in Rat

Male Sprague-Dawley rats (150 - 175g at delivery; Harlan, Dublin, VA) were singly housed in colony rooms maintained at a constant temperature (21 ± 2°C) and humidity (50 ± 10%) and illuminated for 12 h per day (lights on at 0600 h). Behavioral studies were conducted between 0600 and 1300 h. Animals were maintained in accordance with the guidelines of the Animal Care and Use Committee of the Bristol-Myers Squibb Company, the "Guide for Care and Use of Laboratory Animals" and the guidelines published in the National Institutes of Health Guide for the Care and Use of Laboratory Animals. Research protocols were approved by the Bristol-Myers Squibb Company Animal Care and Use Committee.

Rats were food-restricted (15g/rat/day) for 7 days prior to initiation of training and for the duration of the study. Training consisted of 3 days of handling (~5 min per day) followed by 6 days of habituation to the maze. The maze consists of 4 arms (40 cm long x 14 cm wide x 20 cm high) arranged in a '+' configuration and the walls and floor of each arm are distinct and colored either black or white with either a rough or smooth texture (i.e. 1 arm with each of the following combinations: white/smooth, white/rough, black/smooth, black/rough). On the first 4 days of maze habituation, rats were given a single exposure to the maze during which they were placed in the center of the '+' maze and allowed to explore all 4 arms which were each baited with 2 food pellets (45 mg precision pellet, Bio-Serv, Frenchtown, New Jersey). The rats were removed from the maze after consuming all 8 food pellets, placed in a holding chamber for 2 min and then returned to their home cage. The last 2 days of maze habituation were designed to ensure that animals explored the maze with no preference for any particular arm, to prevent positional bias (e.g. always turning right) and to minimize the impact of any extra-maze cues on guiding behavior. For these sessions the maze was set up in a 'T' configuration with 1 arm completely blocked. The arm opposite the blocked arm was designated as the 'start arm' and only 1 of the 2 remaining arms was baited with food pellets. Each animal was given 8 successive trials with a 15 s inter-trial interval during which they were placed in the holding chamber. At the beginning of each trial the animal was placed in the 'start arm' and allowed to visit 1 of the 2 remaining arms and consume the food pellet if the arm was baited. If the animal visited the baited arm (e.g. right arm) then the opposite (i.e. left arm) was baited on the next trial; if not then the arm in the same position (e.g. right) continued to be baited until the pellets had been retrieved. Between successive trials the maze was rotated by 90 degrees so that the adjacent arms now became either the 'start arm' or the arm that was blocked. Thus each arm served as the 'start arm' or 'blocked arm' on 2 out of the 8 trials. Any rat showing >80% side bias (i.e. right or left) was excluded from further testing.

Set shifting was tested following maze habituation and consisted of 2 test sessions conducted over 2 consecutive days. On the first day (Set 1) rats were required to learn the association of either the color or texture of the maze arms with the location of a food reward. Thus, prior to testing each animal was randomly assigned a correct exemplar within a given dimension as being predictive of reward with 50% of the rats assigned color (i.e. black or white) and 50% assigned texture (i.e. rough or smooth). Rats were required to ignore the opposite dimension in order to establish which exemplar within the assigned dimension correctly predicted food at the end of the arm. Each rat was given a maximum of 120 trials on the maze which was configured in the 'T' format and rotated 90 degrees between successive trials as described above. Animals were allowed to visit 1 of the 2 open arms and the trial recorded as correct if the arm with the pre-assigned exemplar was visited and the food reward retrieved. The inter-trial interval was 15 s as previously described. Rats were required to achieve a performance criterion of 8 consecutive entries into the rewarded arm at which point testing stopped and the animal was presumed to have learnt the association between the correct exemplar in the assigned dimension and food reward.

On day 2 (Set 2) animals were again tested in the maze configured as described for Set 1 with the exception that the dimension predicting food reward was now switched (i.e. animals trained on color for Set 1 are now switched to texture and vice versa). Again, within each assigned dimension half the animals were assigned one exemplar as correct (e.g. rough) and half the opposite dimension (e.g. smooth). This new 'correct' assignment requires that the animal suppress previously learned associations that predicted food reward in Set 1 and learn new associations based on correctly establishing the relationship between an exemplar in a different dimension with the presence of food rewards i.e. set shifting. Correct performance was again defined as 8 consecutive entries into the rewarded arm with a maximal number of 80 trials allowed.

The $mGlu_2$ test compound was prepared in 5% DMSO 5% Cremaphor El, 90% saline; add DMSO, vortex; add cremaphor, glass beads and shake overnight; in the morning add saline, let shake 20-30 min. Animals were dosed prior to Set 2 with either mGluR2 test compound (1.0 – 10 mg/kg, po) or vehicle (1 ml/kg, sc) followed 25 min later by either MK-801 (0.04 mg/kg, ip) or vehicle (1 ml/kg, ip) and behavioral testing initiated 35 min later (i.e. 60 min post-treatment with mGluR5 test compound). For comparison, animals dosed with the α7 nACh receptor partial agonist SSR-180711 (10 mg/kg, po; 60 min pretreatment time prior to MK-801) were also included.

Behavioral data were analyzed by analysis of variance followed by a planned contrasts post-hoc test. Statistics were performed using SAS (Statistical Analysis Software, V9.1) with significance set at $p<0.05$.

References and notes

1. Regier, D.A.; Narrow, W.E.; Rae, D.S.; Manderscheid, R.W.; Locke, B.Z.; Goodwin, F.K. *Arch. Gen. Psychiatry*. **1993**, *50*, 85.
2. Wu, E.Q.; Birnbaum, H.G.; Shi, L.; Ball, D.E.; Kessler, R.C.; Moulis, M.; Aggarwal, J. *J. Clin. Psychiatry*. **2005**, *66*, 1122-1129.
3. Sommer, I.E.; Beardon, C.E.; van Dellen, E.; Breetvelt, E.J.; Duijff, S.N.; Maijer, K.; van Amelsvoort, T.; de Hann, L.; Gur R.E.; Arango, C.; Díaz-Caneja, C.M.;

Vinkers, C.H.; Vorstman, J.A.S. *npj Schizophrenia*, **2016**, *2*, 1-9.

4. Pantelis, C.; Yucel, M.; Wood, S.J.; McGorry, P.D.; Velakoulis, D. *Aust N Z J Psychiatry*. **2003**, *37*, 399-406.
5. Newcomer, J.W. *CNS Drugs*, **19**, 1-93.
6. Üçok, A.; Gaebel, W. *World Psychiatry*, **2008**, *7*, 58-62.
7. Krystal, J.H.; Karper, L.P.; Seibyl, J.P.; Freeman, G.K.; Delaney, R.; Bremner, J.D.; Heninger, G. R; Bowers, Jr., M.B.; Charney, D.S. *Arch Gen Psychiatry*. **1994**, *51*, 199-214.
8. Olney, J.W.; Newcomer, J.W.; Farber, N.B. *Journal of Psychiatric Research*. **1999**, *33*, 523-533.
9. Lindsley, C.W.; Emmitte, K.A.; Hopkins, C.R.; Bridges, T.M.; Gregory, K.J.; Niswender, C.M.; Conn, P.J. *Chem.Rev*. **2016**, *116(11)*, 6707-6741.
10. Lilly Stops Phase III Development of Pomaglumetad Methionil for the Treatment of Schizophrenia Based on Efficacy Results (Press Release). Eli Lilly and Company, Aug 29, 2012; available at https://investor.lilly.com/releasedetail.cfm?ReleaseID=703018 (accessed May 3, 2016).
11. Urwyler, S. *Pharmacological Reviews*. **2011**, *63(1)*, 59-126.
12. Ellaithy, A.; Younkin, J.; González-Maeso, J.; Logothetis, D.E. *Trends in Neurosciences*. **2015**, *38(8)*, 506-516.
13. Szabó, G.; Keserű, G.M. *Current Topics in Med. Chem.* **2014**, *14(15)*, 1771-1788.
14. Cook, D.; Brown, B.; Alexander, R.; March, R.; Morgan, P.; Satterthwaite, G.; Pangalos, M.N. *Nature Reviews Drug Discovery*, **2014**, *13*, 419-431.
15. Litman, R.E.; Smith, M.A.; Doherty, J.; Cross, A.; Raines, S. AZD8529, a positive allosteric modulator at the mGluR2 receptor, does not improve symptoms in schizophrenia; a proof of principle study. *Presented at NCDEU an annual meeting of ASCP.* (2014), 16-19 June 2014, Florida.
16. Lavreysen, H.; Langlois, X.; Donck, L.V.; Nuñez, J.M.C.; Pype, S.; Lütjens, R.; Megens, A. *Pharmacology Research and Perspectives*, **2015**, *3(2)*, 1-14.
17. Lavreysen, H.; Ahnaou, A.; Drinkenburg, W.; Langlois, X.; Mackie, C.; Pype, S.; Lütjens, R.; Le Poul, E.; Trabanco, A.A.; Nuñez, J.M.C. *Pharmacology Research and Perspectives*, **2015**, *3(1)*, 1-15.
18. De Boer, P.; Sinha, V.; Hoeben E.; Anghelescu, I-G.; Kezic, I.; Daly, E.; Ceusters, M.; De Smedt, H.; Van Neuten, L.; Kent, J.M. (2013). Characterization of the clinical effect of a positive allosteric modulator of the metabotropic glutamate receptor-2. *68th Annual Scientific Convention of Society of Biological Psychiatry*, May 16-18, 2013, San Francisco, CA.
19. Andrés, J-I.; Alcázar, J.; Cid, J.M.; De Angelis, M.; Iturrino, L.; Langlois, X.; Lavreysen, H.; Trabanco, A.A.; Celen, S.; Bormans, G. *J. Med. Chem*., **2012**, *55*, 8685-8699.
20. Van Laere, K.V.; Koole, M.; de Hoon, J.; Van Hecken, A.; Langlois, X.; Andres, J.I.; Bormans, G.; Schmidt, M. *J Nucl Med*. **2012**; *53 (Supplement 1)*, 355.
21. Cid-Nuñez, J.M.; Trabanco-Suarez, A.A.; Ramiro, V.; Antonio, J.; Oehlrich, D.; Tresadern, G.J.; Macdonald, G.J. WO 2012/062759, 2011.
22. Cid, J.M.; Tresadern, G.; Vega, J.A.; de Lucas, A.I.; Matesanz, E.; Iturrino, L.; Linares, M.L.; Garcia, A.; Andrés, J.I.; Macdonald, G.J.; Oehlrich, D.; Lavreysen, H.; Megens, A.; Ahnaou, A.; Drinkenburg, W.; Mackie, C.; Pype, S.; Gallacher, D.; Trabanco, A.A. *J. Med. Chem*. **2012**, *55*, 8770-8789.
23. Full crystallographic data have been deposited to the Cambridge Crystallographic Data Center (CCDC reference number 1508842). Copies of the data can be obtained free of charge via the internet at www.ccdc.cam.ac.uk/.
24. Full crystallographic data have been deposited to the Cambridge Crystallographic Data Center (CCDC reference number 1508841). Copies of the data can be obtained free of charge via the internet at www.ccdc.cam.ac.uk/.
25. Lavreysen, H.; Langlois, X.; Ahnaou, A.; Drinkenburg, W.; Te Riele, P.; Biesmans, I.; Van der Linden, I.; Peeters, L.; Megens, A.; Wintmolders, C.; Cid, J.M.; Trabanco, A.A.; Andrés, J.I.; Dautzenberg, F.M.; Lütjens, R.; Macdonald, G.; Atack, J.R. *The Journal of Pharmacology and Experimental Therapeutics*. **2013**, *346*, 514-527.
26. Unable to determine a maximal fold shift as apparent desensitization occurred at higher compound concentrations.
27. Pardridge, W.M. *The Journal of the American Society for Experimental NeuroTherapeutics*. **2005**, *2*, 3-14.
28. Bodnar, A.L.; Cortes-Burgos, L.A.; Cook, K.K.; Dinh, D.M.; Groppi, V.E.; Hajos, M.; Higdon, N.R.; Hoffmann, W.E.; Hurst, R.S.; Myers, J.K.; Rogers, B.N.; Wall, T.M.; Wolfe, M.L.; Wong, E. *J. Med. Chem*. **2005**, *48*, 905-908.
29. Jones, K.M.; McDonald, I.M.; Bourin, C.; Olson, R.E.; Bristow, L.J.; Easton, A. *Psychopharmacology*. **2014**, *231*, 673-683.
30. Biton, B.; Bergis, O.E.; Galli, F.; Nedelec, A.; Lochead, A.W.; Jegham, S.; Godet, D.; Lanneau, C.; Santamaria, R.; Chesney, F.; Leonardon, J.; Granger, P.; Debono, M.W.; Bohme, G.A.; Sgard, F.; Besnard, F.; Graham, D.; Coste, A.; Oblin, A.; Curet, O.; Vige, X.; Voltz, C.; Rouquier, L.; Souilhac, J.; Santucci, V.; Guedet, C.; Francon, D.; Steinberg, R.; Griebel, G.; Oury-Donat, F.; George, P.; Avenet, P.; Scatton, B. *Neuropsychopharmacology*. **2007**, *32 (1)*, 1-16.
31. MacroModel, Schrödinger, LLC: Portland, OR. (2016).
32. Cid-Nuñez, J.M.; de Lucas O.A.I.; Trabanco, A.A.; Macdonald, G.J. WO 2010/130422, 2009.
33. Redrobe, J.; Nielson, E.; Christensen, J.; Peters, D.; Timmermann, D.B.; Olsen, G.M.; *Eur J Pharmacol*. **2009**, *602(1)*, 58-65.

Graphical Abstract

To create your abstract, type over the instructions in the template box below.
Fonts or abstract dimensions should not be changed or altered.

Triazolopyridine Ethers as Potent, Orally Active mGluR2 Positive Allosteric Modulators for Treating Schizophrenia

Leave this area blank for abstract info.

Mendi A. Higgins*, Lawrence R. Marcin, F. Christopher Zusi, Robert Gentles, Min Ding, Bradley C. Pearce, Amy Easton, Walter A. Kostich, Matthew A. Seager, Clotilde Bourin, Linda J. Bristow, Kim A. Johnson, Regina Miller, John Hogan, Valerie Whiterock, Michael Gulianello, Meredith Ferrante, Yanling Huang, Adam Hendricson, Andrew Alt, John E. Macor, Joanne J. Bronson

Bristol-Myers Squibb, Research and Development, 5 Research Parkway, Wallingford, CT 06492-7660, USA

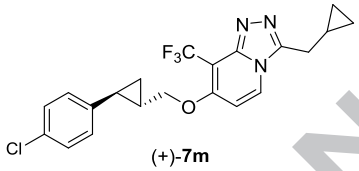

(+)-**7m**